

Shear Behavior of Expanded Polystyrene Geofoam (An Experimental Investigation)

Mamdouh Eldamarawy^{1,*}, Mohamed Medhat², Mohammed Rabie³, Hussein Mostafa⁴

¹ Assistant lecturer, Faculty of Engineering at Mataria branch, Helwan University, Cairo, Egypt

² Researcher, Construction Research Institute, National Water Research Centre, Egypt, El Qalyubia, Egypt

³ Professor of Geotechnical Engineering, Faculty of Engineering at Mataria branch, Helwan University, Cairo, Egypt

⁴ Lecturer, Faculty of Engineering at Mataria branch, Helwan University, Cairo, Egypt

*Corresponding author E-mail: Mamdouh.eldamarawy@m-eng.helwan.edu.eg

Abstract. Expanded polystyrene geofoams (EPS) have gained importance in geotechnical engineering applications since 1960s. These materials serve multiple purposes, such as lightweight fills in the construction of structures, embankments, and bridges, as well as compressible inclusions in culverts and retaining walls. Most of these applications, geofoams are placed directly with other geofoam elements or other construction materials. A key challenge in designing such systems is to understand how geofoams interact with other construction materials. This requires an intensive examination of the shear strength behavior of geofoam, in addition to the shear strength interfaces with other materials such as geofoam, sand, concrete, and steel. The aim of this study is to determine the shear strength parameters of EPS geofoam blocks with different densities of 25, 30, and 35 kg/m³. To achieve this, multiple direct shear tests were conducted, which provided vital information regarding material performance. The findings proved a distinct relationship between density and shear behavior: a higher geofoam density corresponded to increased material cohesion and internal friction angle. This study also investigated the interface shear strength between EPS geofoam versus other construction materials for instance sand, geofoam, concrete, and steel. These experimental results provide valuable information for geotechnical engineers, allowing for more accurate analytical and numerical modeling of EPS–material structure interactions.

Keywords: EPS Geofoam, Friction Angle, Cohesion, Direct Shear test, Interface Strength.

1 Introduction

Expanded polystyrene (EPS) is characterized as a lightweight, rigid cellular foam that exhibits a significantly lower density compared to conventional backfill materials. The development of EPS was

attributed to Germany during the mid-20th century. The effectiveness of geofoam blocks has been proven in a variety of geotechnical engineering settings. In addition to being lightweight fill components, these materials also operate as barriers to vibrations and offer seismic protection for rigid structural systems [1]. The placement of geofoam inclusions above underground pipes, buried culverts, or behind retaining walls has been demonstrated to lower the earth loads on these structures, resulting in designs that are both secure and economically efficient [2], [3], [4]. Although geofoam blocks in these applications typically experience compressive forces, the interplay between the protected structure and the surrounding soil may generate shear stresses. This is particularly true when geofoam is placed towards the sidewalls of the structure [5]. In geotechnical engineering applications, EPS geofoam is frequently utilized and often comes into direct contact with a variety of materials. These materials include soil, steel, geotextiles, and concrete. Hence, the effective design of such structures necessitates a comprehensive understanding of the geofoam shear characteristics and durability of their interfaces. Researchers have extensively investigated the strength properties of geofoam blocks, as well as the interface characteristics that develop when geofoam interacts with various construction materials or itself. Shear deformations within EPS geofoam blocks typically exhibit along a horizontal plane that emerges through the material. In contrast, when a normal force is applied, interface shear failure takes place along the surface of contact[5]. The following section provides a summary of various experimental investigations on the shear behavior of interfaces and the shear strength of geofoam blocks.

1.1 Shear Strength of Geofoam Blocks

Studies conducted by [1] on geofoam specimens with varying densities demonstrated that the cohesive shear strength increased in direct proportion to the density of the material. Comparable results were observed in a study by [6], who performed direct shear tests on different geofoam blocks, which had densities varying between 15 and 30 kg/m³. The findings showed that increasing the density of geofoam substantially enhanced the cohesion and marginally improved the angle of internal friction. In addition, [7] carried out direct shear experiments on EPS specimens with typical stress levels between 10 and 40 kPa showed that adhesion and friction coefficients both affect the interface shear strength, while cohesion is the main factor affecting the shear strength of geofoam blocks. An overview of the shear strength characteristics of the EPS blocks is presented in Table 1. This research offers recommendations for calculating the EPS geofoam blocks' shear strength parameters.

Table 1. Chosen studies of EPS geofoam.

Ref.	Size of the sample (mm × mm)	EPS density (kg/m ³)	Shear strength parameters	
			C (KPa)	φ (°)
[1]	—	18.4	27.5	—
		28.8	50	—
[6]	100 × 100	15	30.8	3
		20	36	4
		22	40.3	4.5
		30	59.8	6
[7]	100 × 100	18.5	26.6	10
		29.9	49.8	8.9

1.2 Geofoam Shear Interface Behavior

The interface shear behavior of expanded polystyrene geofoam can be classified into three distinct categories: interactions between geofoam layers, geofoam–sand interactions, and geofoam in contact

with various materials, including concrete, steel, and geotextiles. The following section presents the relevant literature on these categories.

A study utilized two blocks of geofoam with a density of 22 kg/m^3 , and experiments were conducted to assess the strength of the interface between these blocks [8]. The findings were analyzed with those from the direct shear tests. Tests revealed a geofoam–geofoam friction coefficient of 0.54, while direct shear tests showed peak and residual interface friction coefficients of 0.63 and 0.52, respectively. Experiments using a shaking table were performed to evaluate the interface strength between geofoam layers and to investigate the impact of binder plates inserted between block layers under both static and dynamic loading conditions. These tests applied normal stresses of 7.5 and 14.8 kPa to assess the geofoam-geofoam interaction. Measurements revealed that the interface friction coefficients fell within the range of 0.2 to 0.4 [9]. The effects of water on the interface characteristics between geofoam layers were investigated [10]. The study discovered that variables including working stress level, geofoam density, and surface moisture had minimal effects on the interface properties. Direct shear tests performed by [11] on geofoam specimens utilizing barbed connector plates and those without, subjected to different normal stress levels, demonstrated that the incorporation of barbed connector plates failed to enhance the interfacial shear resistance.

Research by [12] using direct shear tests showed that the coefficients of interface friction varied from 0.55 to 0.7 between geofoam and sand, depending on the thickness of the sand layer beneath the geofoam. The friction coefficient of the geofoam-sand interface is comparable to that of sand itself [13]. Three stages were identified in the geofoam-sand interaction mechanism: frictional only, frictional-adhesion, and adhesion only, which depend on the applied normal stress [14].

Tests of direct shear were conducted on geofoam interfaces with cast-in-place concrete and geomembranes [10]. Their results indicated that the geofoam-cast-in-place concrete interface provides greater friction than the geofoam-geomembrane interface, with both cases exhibiting peak and residual responses. The coefficient of interface friction observed between geofoam and various materials, including geotextiles, geomembranes, soils, and both cast in place and precast concrete, varied from 0.28 to 1.22 [15]. A complementary investigation by [16] analyzed the characteristics of geofoam interfaces when in contact with various construction materials, including geogrid, fly ash, and geotextile. They observed that increasing the density of the geofoam led to a slight increase in the adhesion values, whereas the interface friction angle remained constant. Experimental results involving geofoam-steel interfaces utilizing EPS samples with different densities were presented by [5]. The results showed that the geofoam-steel interface varied from 0.5 to 0.67.

Table 2 provides an overview of the available interface friction coefficients. The research conducted provides an understanding of determining the shear characteristics of geofoam blocks and the interface strength between geofoam and various materials under different test conditions. The recommendations for the interface coefficients varied. Since the Norwegian Road Research Laboratory [17] suggested a coefficient of 0.7 can be adopted in the calculation of the interface between the geofoam-geofoam and geofoam-sand. While the UK Transportation Research Laboratory [18] proposed an internal coefficient of 0.5 between the geofoam-geofoam.

Despite the increasing use of underground structures in geotechnical applications in recent years, there has been limited research on the interface shear parameters of EPS geofoams in contact with these structural materials. This study aims to address this gap by experimentally investigating the shear behavior of EPS geofoam blocks with densities ranging from 25 to 35 kg/m^3 and measuring the parameters of interface strength of EPS blocks in contact with geofoam, sand, concrete, and steel materials.

Table 2. Selected investigations of geofoam interface.

Interface type	Ref.	Size of sample size (mm × mm)	Geofoam density (kg/m ³)	Coefficient of friction
Geofoam to Geofoam	[10]	100 × 100 to 500 × 500	18	0.9 (peak) 0.7 (residual)
	[11]	430 × 280 × 100	15	0.60–0.99 (peak) 0.60–0.75 (residual)
			30	0.87–1.06 (peak) 0.74–0.86 (residual)
Geofoam to Sand	[12]	-	20	0.70 (thickness of sand layer < 35 mm) 0.55 (thickness of sand layer > 35 mm)
	[13]	100 × 100	-	1
	[14]	100 × 100	10	0.67 (frictional) 0.35 (frictional–adhesion) 0 (adhesion)
			20	0.63 (frictional) 0.28 (frictional–adhesion)
Geofoam to Concrete	[10]	100 × 100 × 25	-	2.36 (peak), 1 (residual)
Geofoam to other materials (geotextile, geomembrane, fly ash)	[15]	100 × 100	20	0.27 to 1.2
	[16]	300 × 300 × 75	15	0.17 to 0.21
			30	0.19 to 0.23
Geofoam to Steel	[5]	100 × 100 × 50	15, 22, and 39	0.5 to 0.67

2 Experimental Program

To assess the behavior of shear strength and interface of the geofoam with various materials, an intensive direct shear test program was conducted. This study examined three EPS geofoam densities 25, 30, and 35 kg/m³ in combination with geofoam, sand, concrete, and steel. In total, 67 tests were

conducted, comprising of twelve (12) tests on geofoam blocks, seven (7) tests on sand samples, and 48 interface shear tests. The interface tests involved the aforementioned materials (sand, geofoam, concrete, and steel), and each test was repeated four times with different normal stresses for each geofoam density. The following section provides a concise overview of the material properties and the testing methodology.

2.1 Material Properties

This study utilized various materials including EPS geofoam, sand, concrete, and steel. Geofoam specimens were extracted from three large blocks with densities of 25 (EPS 25), 30 (EPS 30), and 35 kg/m³ (EPS 35), representing the typical ranges used in geotechnical applications. According to the manufacturer (INSUTECH), the EPS densities exhibited compressive strengths of 150, 200, and 250 kPa at 10 % strain for EPS 25, 30, and 35, respectively. The compressive strength was determined according to EN-826 [19]. The used EPS geofoam block dimensions are 99.5 mm × 99.5 mm × 25 mm in Fig. 1. While the geofoam samples used for the interface tests had dimensions of 99.5 mm × 99.5 mm × 10 to 17 mm.

To create the concrete block, a concrete mixture was prepared using locally sourced materials (sand, ordinary Portland cement, and potable water). The mixture was prepared and poured into a wooden mold with dimensions of 99 mm × 99 mm × 15 mm. The mold was designed to fit the bottom half of the shear box, as illustrated in Fig. 1. A steel sample was precisely sliced to fit the lower section of the direct shear box.

According to the sieve analysis test conducted on sand, Coarse-to-fine silica sand was used in this study since this is the typical material used as a backfill material. Using a vibratory table, the highest and lowest dry unit weights of the sand specimens were determined in compliance with ASTM D4254 [20]. The grain size distribution curve of the sand is shown in Fig. 2. The particle size distribution curve of the used sand and the index parameters are presented in Table 3.

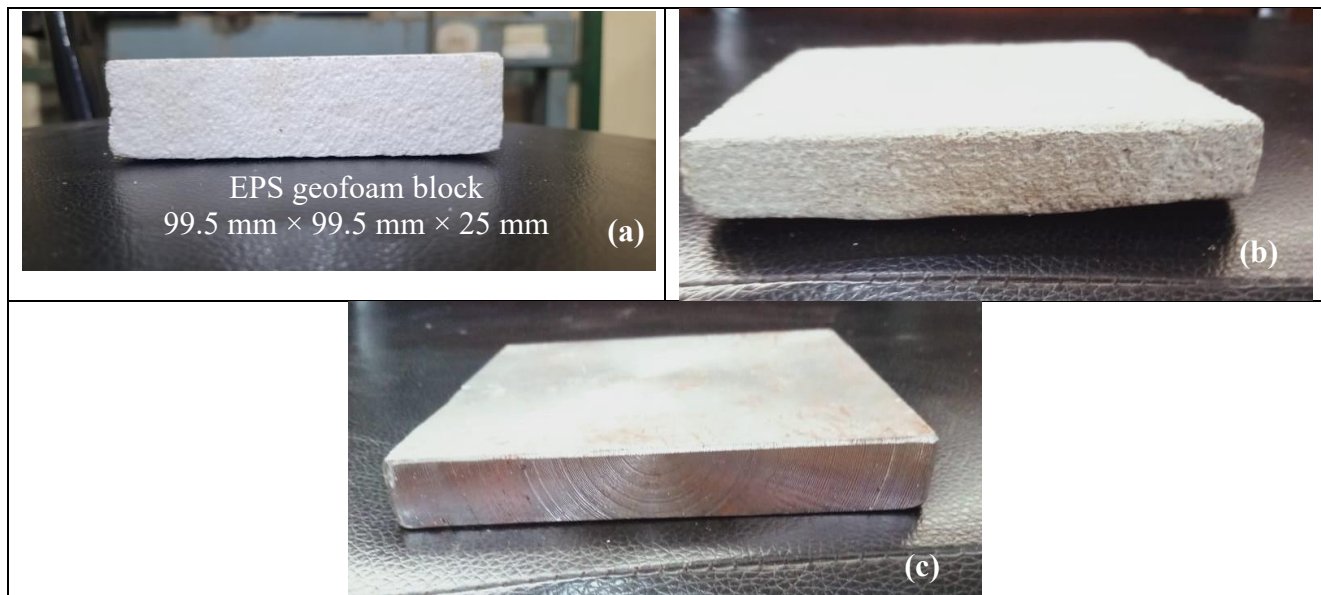


Fig. 1. Tested material: (a) EPS geofoam block; (b) concrete block; (c) steel block

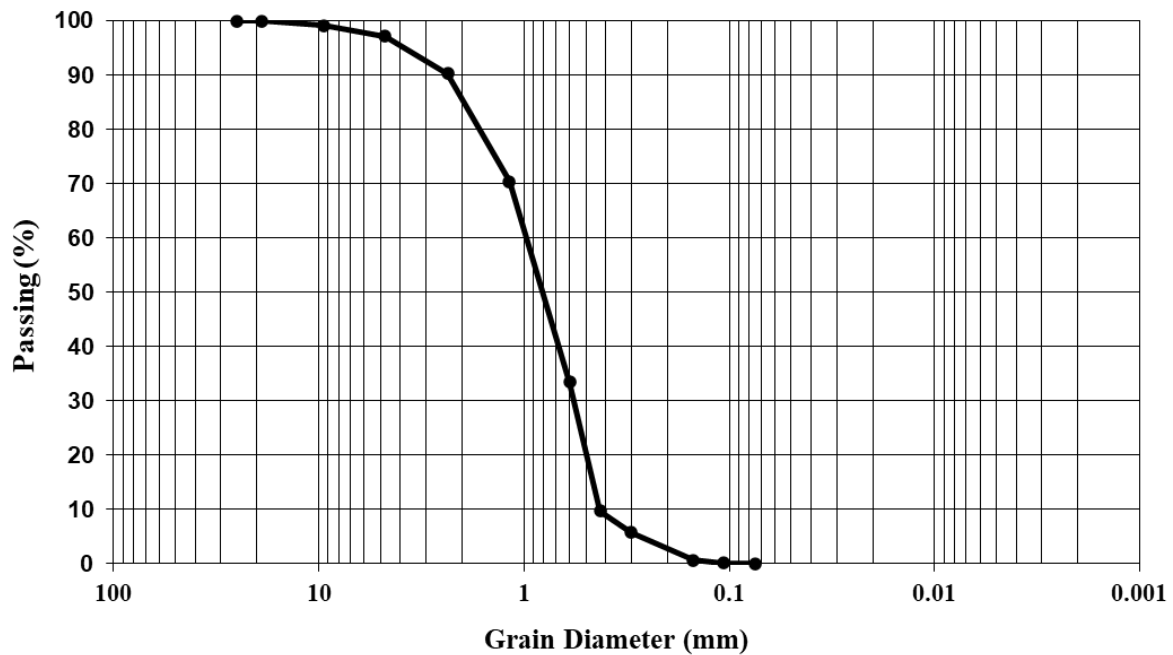


Fig. 2. Particle size distribution curve of the used sand.

Table 3. Properties of the sand.

Parameter	Value
D ₁₀	0.45
D ₃₀	0.6
D ₆₀	1
Uniformity coefficient, C_u	2.2
Coefficient of curvature, C_c	0.8
Classification according to ASTM D2487 [21]	SP
γ_{\max} (gm/cm ³)	1.83
γ_{\min} (gm/cm ³)	1.53

2.2 Test Procedure

Four distinct normal stresses were applied: 8.8, 20, 30, and 42 kPa. The tests were concluded upon reaching a maximum displacement of approximately 10 mm, which was a limit imposed by the horizontal movement capacity of the direct shear device. This study employed the shear box measuring 100 mm × 100 mm × 50 mm, with tests conducted following ASTM D5321 [22]. Four distinct normal stresses were applied: 8.8, 20, 30, and 42 kPa. A horizontal displacement rate of 0.84 mm/min was utilized. Fixed dial gauges with 0.01 mm precision were used to monitor both horizontal and vertical displacements. The tests were concluded upon reaching a maximum displacement of approximately 10 mm, which was the limit imposed by the horizontal movement capacity of the direct shear apparatus. According to the ASTM D3080 [23] guidelines, in the absence of an observable peak response, the peak shear could be considered to occur at 10 % of the horizontal strain. Experiments were conducted on

EPS geofoam blocks with dimensions $99.5 \text{ mm} \times 99.5 \text{ mm} \times 25 \text{ mm}$ (see Fig. 1). This study encompassed 12 tests, with four tests performed for each EPS geofoam density under investigation. The shear interface tests were used to evaluate geofoam in direct contact with various materials, including sand, geofoam, concrete, and steel. During these tests, the geofoam was positioned in the upper part of the shear box, whereas the other material samples occupied the lower half. This configuration was chosen because concrete and steel were deemed incompressible relative to the geofoam under the applied loads. This setup ensured that the surface of the shear remained aligned with the dividing plane between the lower and upper sections of the shear box. To investigate the interface between geofoam and sand, a similar experimental arrangement was used. The lower section of the box was filled with sand, which was then compacted to reach a target density of 1.8 g/cm^3 , which is equivalent to 95 % of the relative density of sand. Subsequently, the EPS geofoam block was placed on top of the compacted sand layer.

3 Results and Discussion

For each experiment, the applied normal and shear forces along with their corresponding displacements were measured. These experimental outcomes were utilized to get the failure envelopes and establish the shear strength parameters for the settings under investigation. For each experiment conducted, measurements were taken of the applied normal and shear forces, along with their corresponding displacements. It is important to note that EPS geofoam blocks typically do not experience shear failure or rupture along the shear plane. Instead, the initiation of EPS geofoam block shear failure is characterized by an apparent failure or significant permanent deformation (as illustrated in Fig. 3).

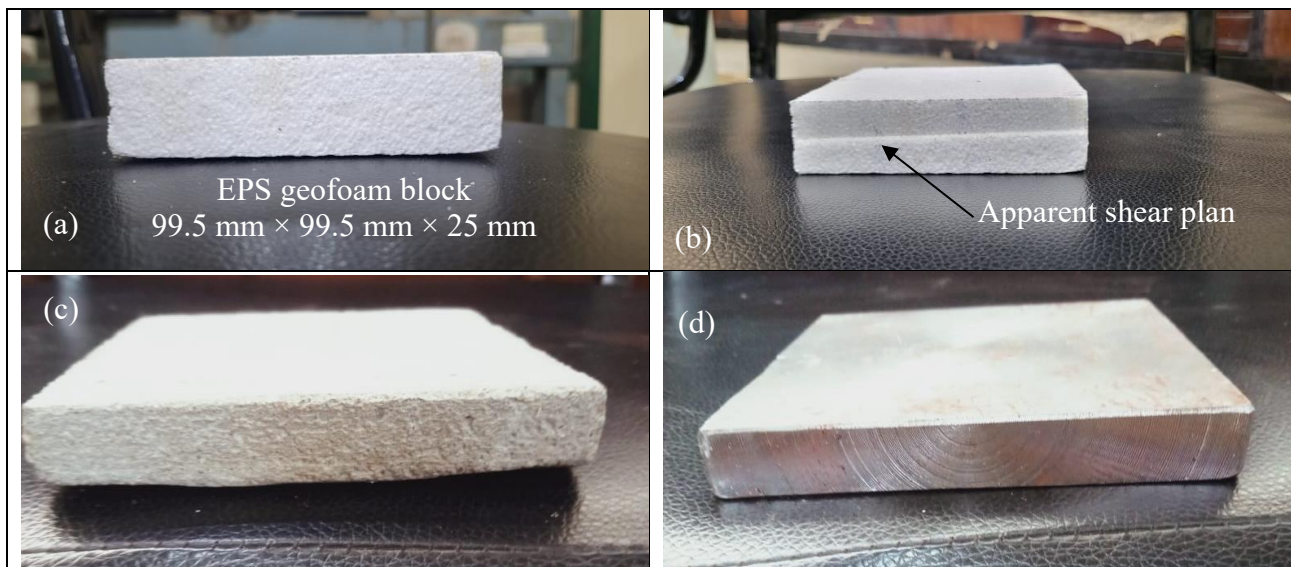


Fig. 3. Tested material: (a) EPS geofoam block before test; (b) EPS geofoam block after test; (c) concrete; (d) steel

3.1 Geofoam Block Shear Strength

The shear strengths, horizontal displacements, and corresponding shear stresses of EPS25, EPS30, and EPS35 geofoam blocks are shown in Fig. 4 to Fig.6. These illustrations present data for normal stress levels of 8.8, 20, 30, and 42 kN/m^2 , showcasing the behavior of each geofoam type under various stress conditions. With increasing displacement, a corresponding increase in shear stress was observed, and no definitive failure pattern was developed throughout the displacement range of up to 10 mm. Response

of geofoam exhibits two phases. Phase one represents the horizontal displacements up to 3 mm, the shear stress increased almost linearly. At a horizontal displacement of 3 mm, the maximum shear stresses were approximately 24, 37, and 38 kPa for EPS25, EPS30, and EPS35, respectively. While phase two, beyond 3 mm horizontal displacement, the shear stress continued to rise at a reduced rate, reaching ultimate values of 32.7, 45.9, and 54 kPa for EPS25, EPS30, and EPS35, respectively. Additionally, it is noted that the shear stress of EPS 30 exhibits almost the same trend for all normal stress except for normal stress, which is equal to 42 Kpa. This could be due to the non-homogeneity of the geofoam material.

The Mohr-Coulomb (M-C) failure envelopes for the three densities of geofoam were created using the measured normal and shear stresses, as illustrated in Fig. 7. These envelopes are generally parallel with slightly upward slopes. Higher geofoam densities were correlated with an increased shear resistance. Research indicates that shear resistance is directly linked to geofoam material cohesion because the shear box induces a horizontal shear plane through the geofoam specimen.

Fig. 8 and Fig. 9 depict the variations in the friction angle and cohesion for the geofoam blocks with varying densities. The cohesive strength increased with density, ranging from 22.74 kPa for EPS25 to approximately 41.40 kPa for EPS35, as shown in Fig. 8. In addition, the angle of friction increased slightly from approximately 13.4° for EPS25 to 16.9° for EPS35, as shown in Fig. 9. These results confirm that material cohesion is the primary determinant of geofoam shear strength. Table 4 summarizes the results of the studied geofoam densities and their shear strength parameters.

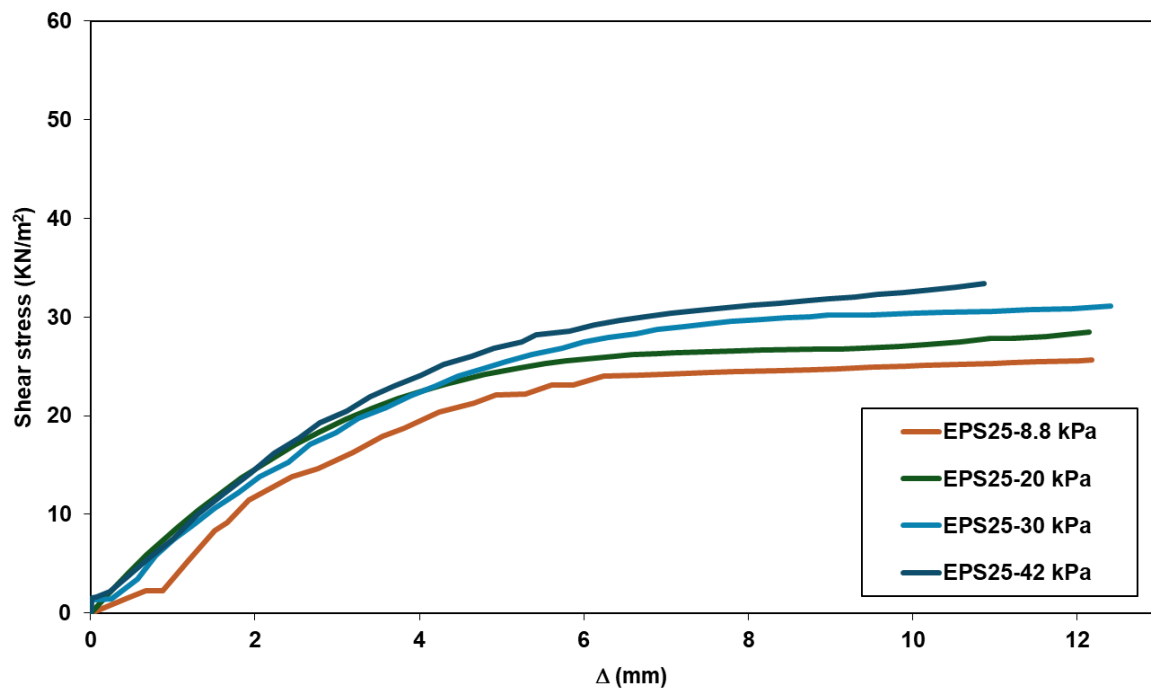


Fig. 4. Shear stresses vs corresponding horizontal displacement for EPS with density 25 (kg/m^3)

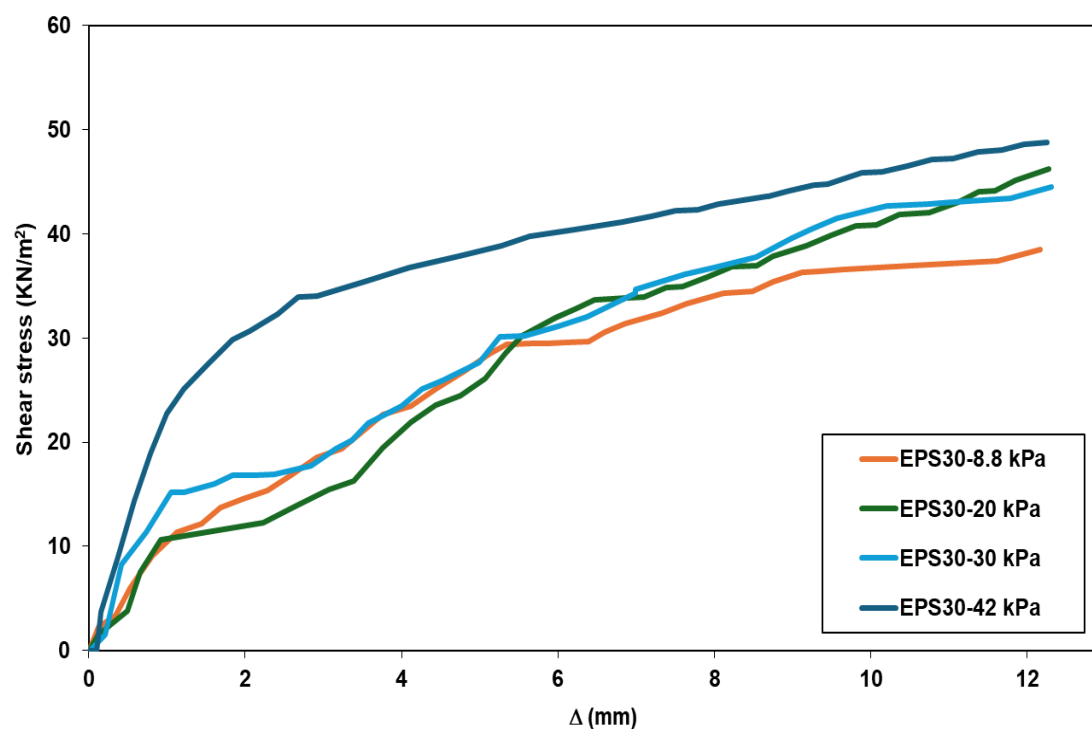


Fig. 5. Shear stresses vs corresponding horizontal displacement for EPS with density 30 (kg/m³)

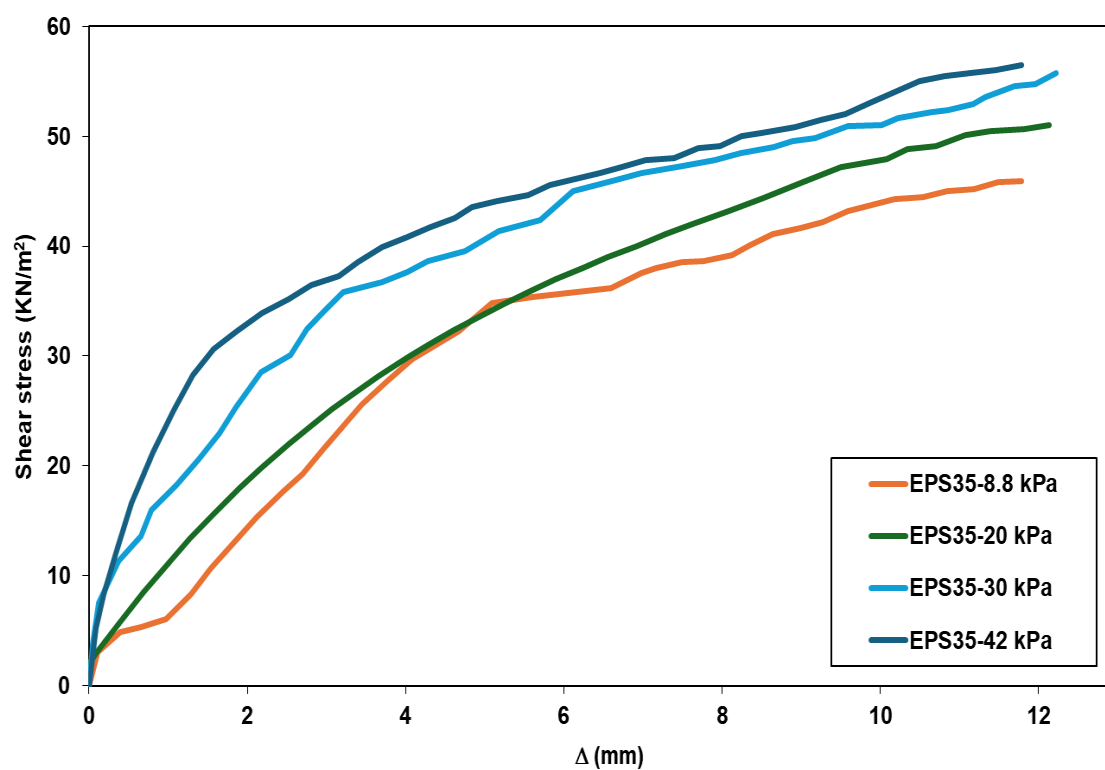


Fig. 6. Shear stresses vs corresponding horizontal displacement for EPS with density 35 (kg/m³)

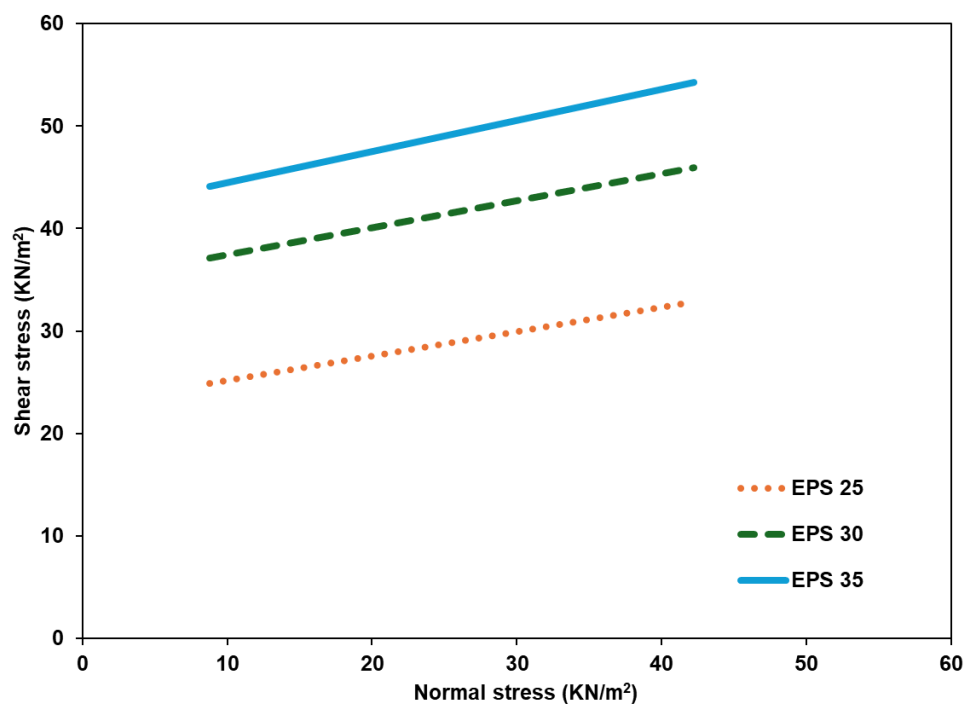


Fig. 7. Failure envelopes of geofoam blocks

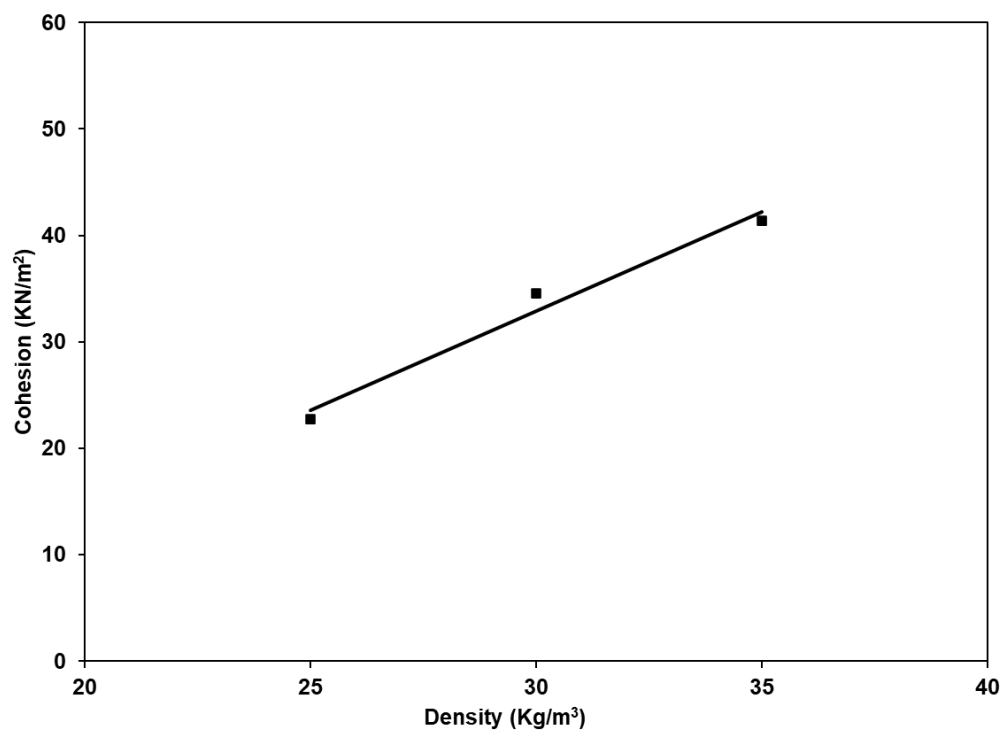


Fig. 8. Relation between geofoam block density and cohesion strength

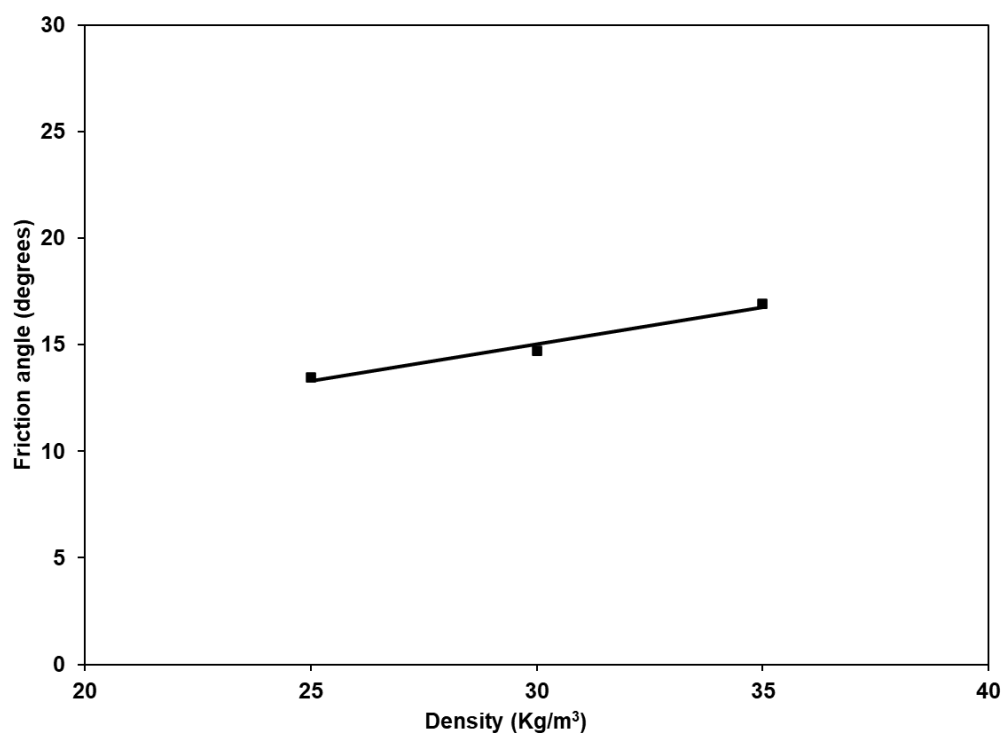


Fig. 9. Relation between geofoam block density and internal friction angle

Table 4. Selected EPS geofoam studies.

Shear box size (mm × mm)	Geofoam density (kg/m³)	Shear strength parameters	
		C (kPa)	ϕ (°)
100 × 100 × 50	25	22.75	13.45
	30	34.58	14.7
	35	41.40	16.9

3.2 Shear Strength of Sand

The parameters of the shear strength of the sand samples were evaluated under a series of normal loads ranging from 8.8 kPa to 114 kPa at 95 % of the sand relative density. Fig. 10 illustrates the lateral movement and associated shear forces. As expected, the shear stress increased with the displacement increased. The measured shear and normal stresses were used to create M-C failure envelopes for sand, as shown in Fig. 11, which reveals that the measured internal friction angle of the sand sample was 37.4°.

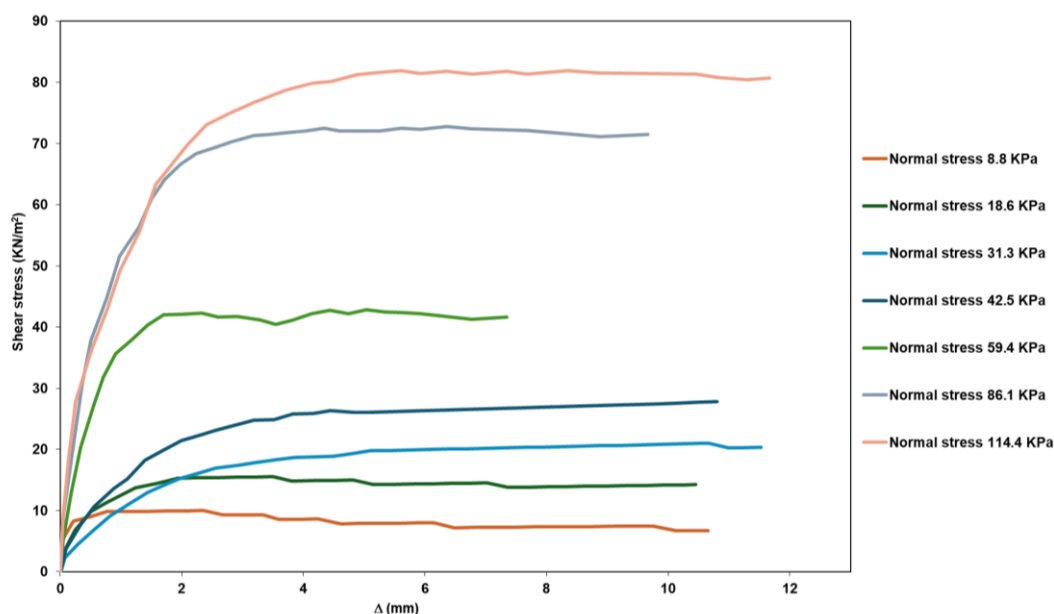


Fig. 10. Shear stresses and corresponding horizontal displacement for sand

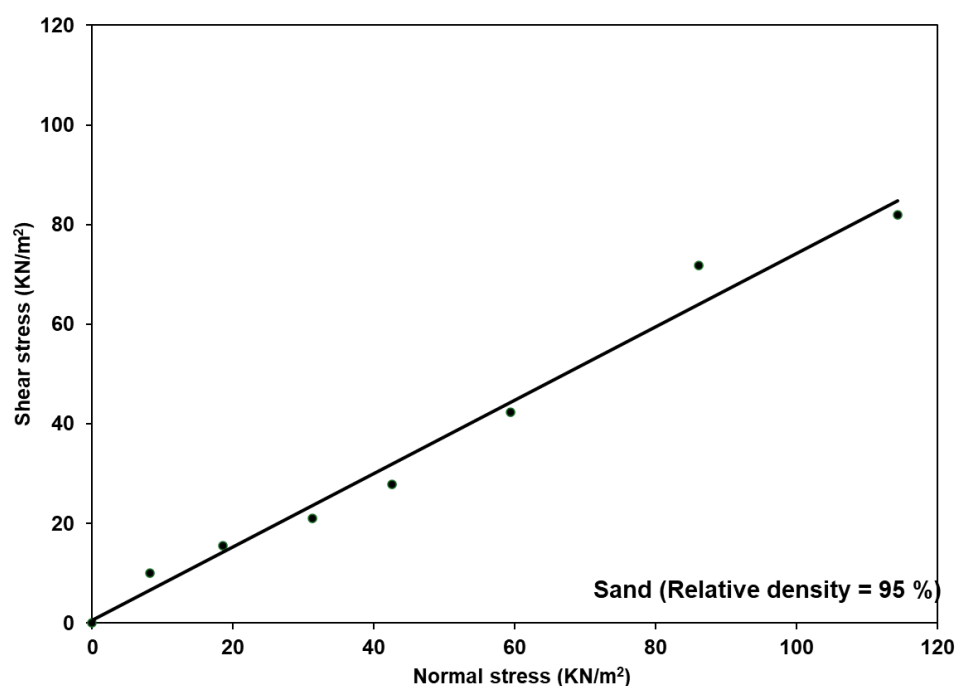


Fig. 11. Failure envelopes of sand sample with a relative density of 95 %

3.3 Geofoam Interface Strength

The results of direct shear tests investigating the shear resistance of geofoam blocks in contact with various materials, including sand, geofoam, concrete, and steel, are presented in this section.

Geofoam – Sand interface

Relations concerning the horizontal displacements versus shear stresses for the interface of geofoam–sand are shown in Fig. 11 to Fig. 13. A rapid increase in the shear stress was observed as the horizontal

displacement increased to approximately 1 mm. At 1 mm horizontal displacement, the average measured shear resistance was 10.9, 11.4, and 11.8 kPa for EPS25, EPS30, and EPS35, respectively. A minor increase in displacement was noted in all instances as the displacement increased from 1 to 2.5 mm, followed by a steady state for displacements exceeding 2.5 mm. None of the three geofoam materials exhibited any peak stress. Fig. 15 shows the M-C failure envelopes developed at the geofoam–sand interface in the present study. The shear stress differences among the three geofoam densities were minimal for both low and high normal stresses. Fig. 16 and 17 show the shear strength parameters for various geofoam densities at the sand interface. As illustrated in Fig. 16, the adhesion values decreased from approximately 4.5 to 0.5 kPa as the density increased from 25 to 35 kg/m³, with an average value of 2.72 kPa. The observed phenomenon could be attributed to the higher stiffness of EPS35 geofoam, which results in reduced interaction with sand particles compared to the softer EPS25. Consequently, this reduced interaction enables the penetration of sand into the contact surface. As shown in Fig. 17, the friction angle increased from 24° for EPS25 to 32° for EPS35, with an average interface friction angle of 29.4°. Examination of the samples after testing revealed that sand particles in the upper layer were forced into the geofoam blocks (EPS25) soft surface during the test, creating a rough surface. Stiffer geofoam blocks (EPS35) demonstrated less interaction with the sand material.

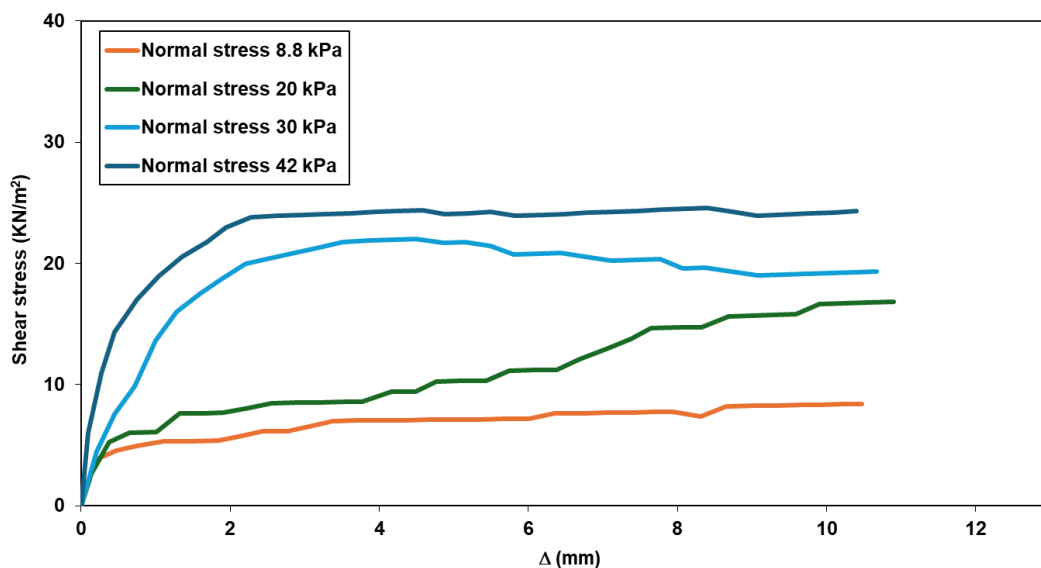


Fig. 12. Shear stresses versus corresponding horizontal displacement for (EPS 25) geofoam–sand interface

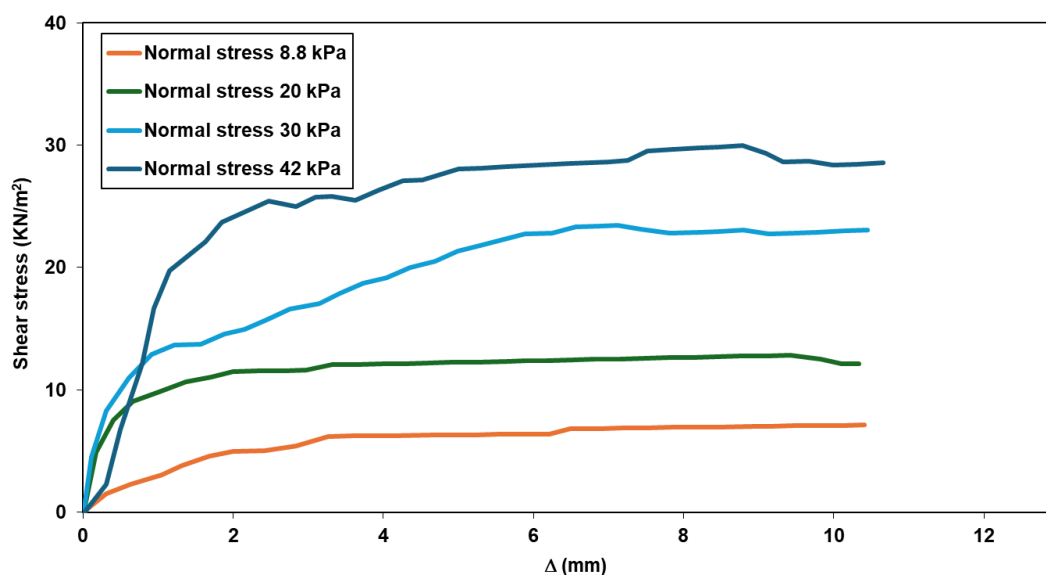


Fig. 13. Shear stresses versus corresponding horizontal displacement for (EPS 30) geofoam-sand interface

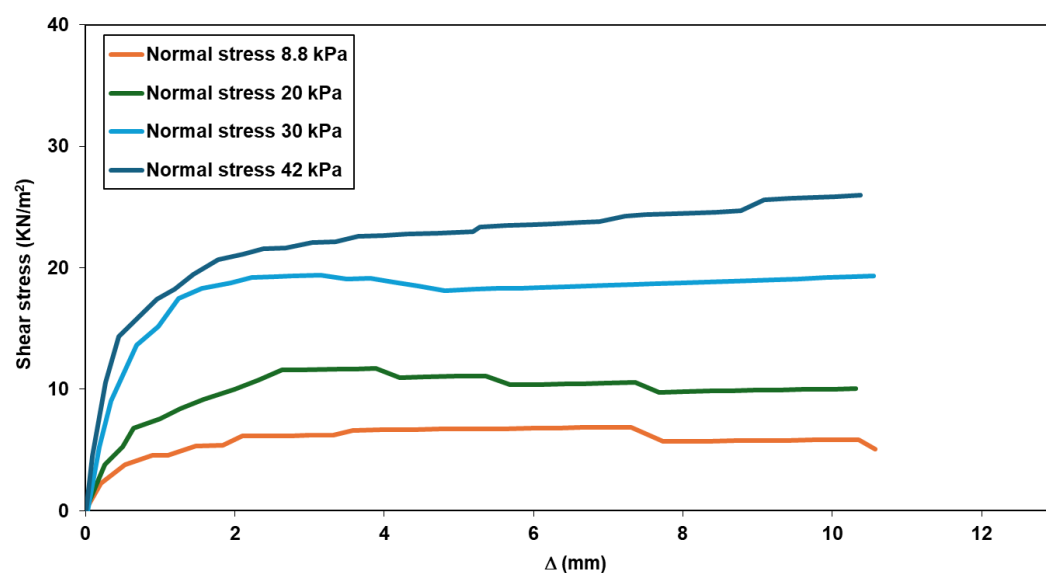


Fig. 14. Shear stresses versus corresponding horizontal displacement for (EPS 35) geofoam-sand interface

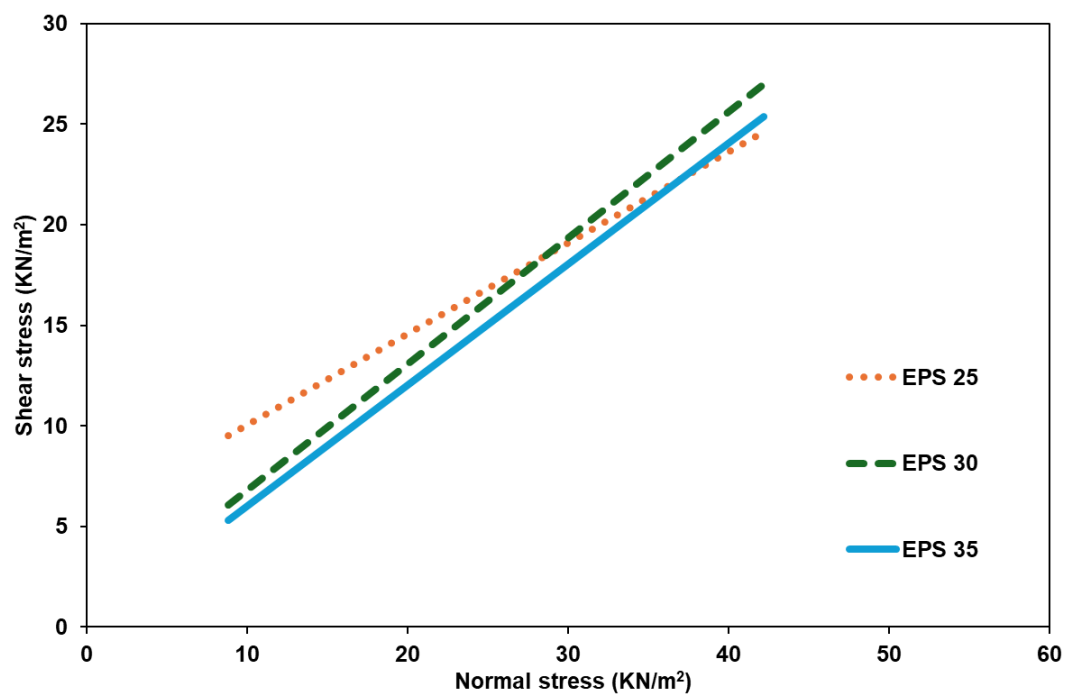


Fig. 15. Failure envelopes of geofoam blocks – sand interface

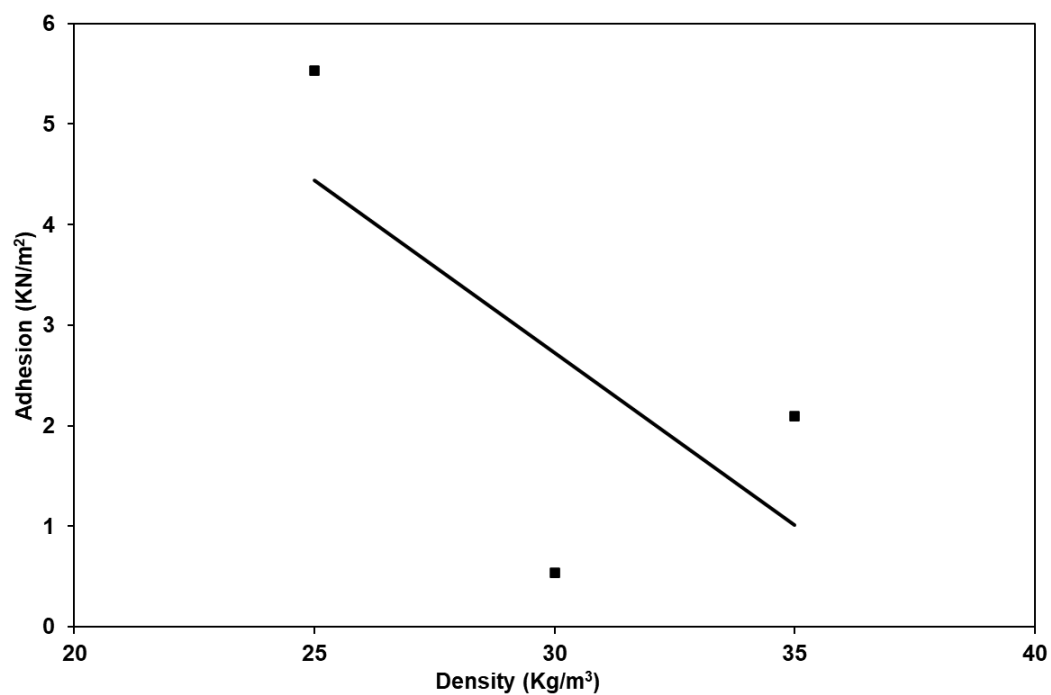


Fig. 16. Relation between geofoam block-sand interface and adhesion strength

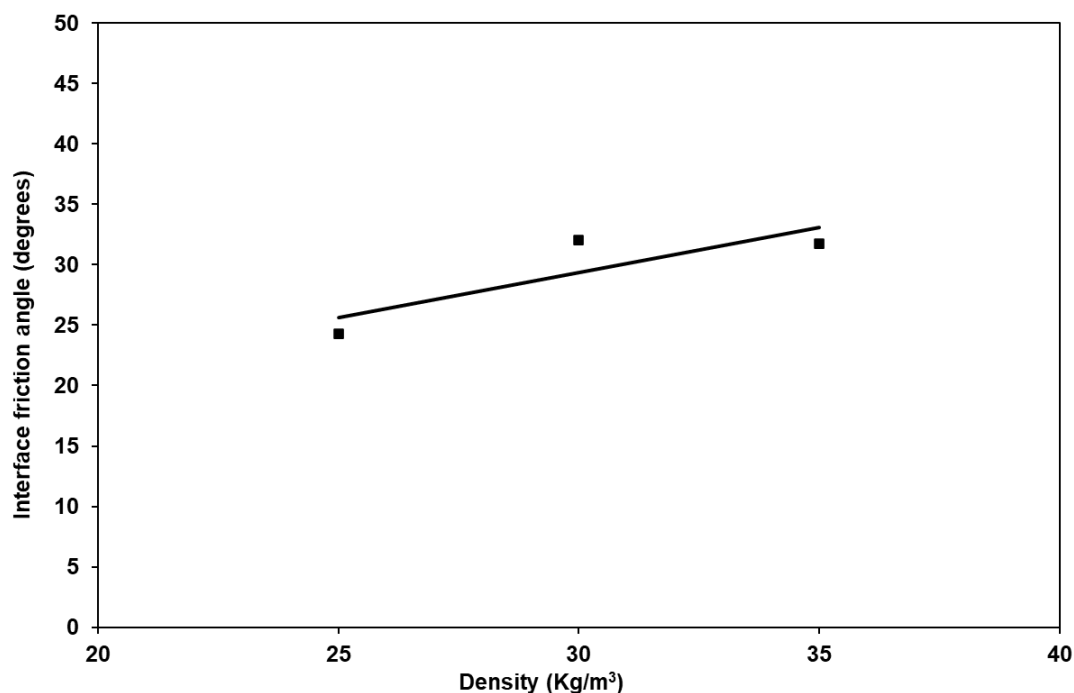


Fig. 17. Relation between geofoam block-sand interface and interface friction angle

Geofoam – Geofoam interface

Fig. 18 through Fig. 20 illustrate the relations between horizontal displacements and shear stresses at the interface of geofoam-geofoam materials. EPS 25 exhibited a gradual increase in shear stress, whereas EPS 30 and 35 exhibited a rapid increase as the horizontal displacement increased. For EPS 25, the shear stress increased to approximately 4 mm before becoming constant. In contrast, EPS 30 and 35 experienced increased shear stress up to 2.5 a of horizontal displacement, followed by a steady-state shear outcome. The average maximum shear stress measured was 27.7, 30.28, and 24.5 kPa for EPS25, EPS30, and EPS35, respectively. Peak stresses were noted in four of the 12 tests, whereas the remaining maximum shear stresses were observed as residual stresses across all three geofoam materials examined. Fig. 21 shows the M-C failure envelopes developed at the interface surface of the geofoam–geofoam. The variation in shear stress among the three geofoam densities was minimal for both low and high normal stresses. Fig. 21 shows the shear strength versus the normal stress for various geofoam-geofoam interfaces. As shown in Fig. 22, the adhesion values rapidly declined from approximately 11.3 to 1.1 kPa as the density increased from 25 to 35 kg/m³, with an average value of 6 kPa. Conversely, Fig. 23 shows that the interface friction angle increased from 32° to 44°, with an internal angle of 39.6°.

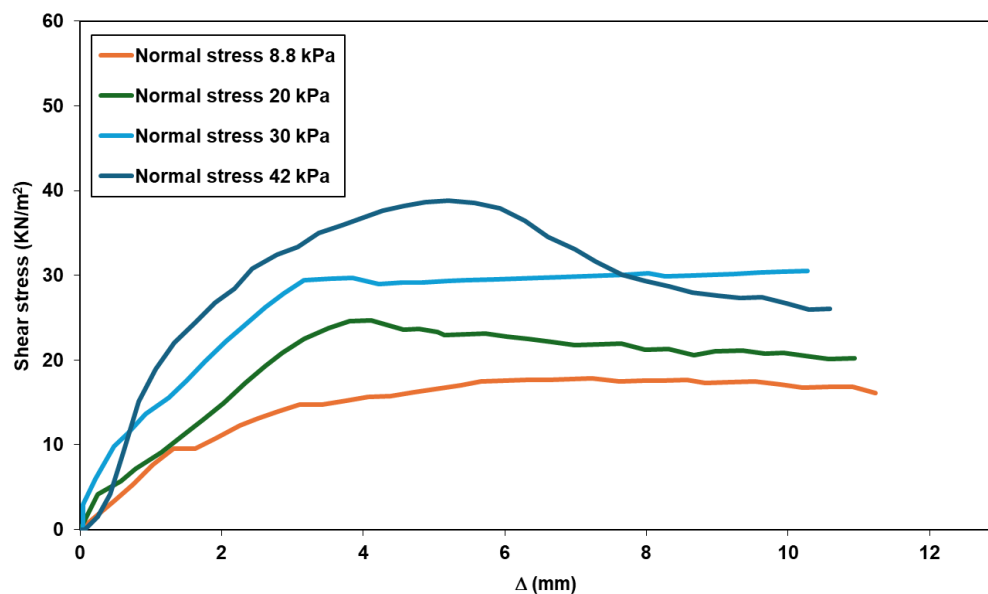


Fig. 18. Shear stresses versus corresponding horizontal displacement for (EPS 25) geofoam–geofoam interface

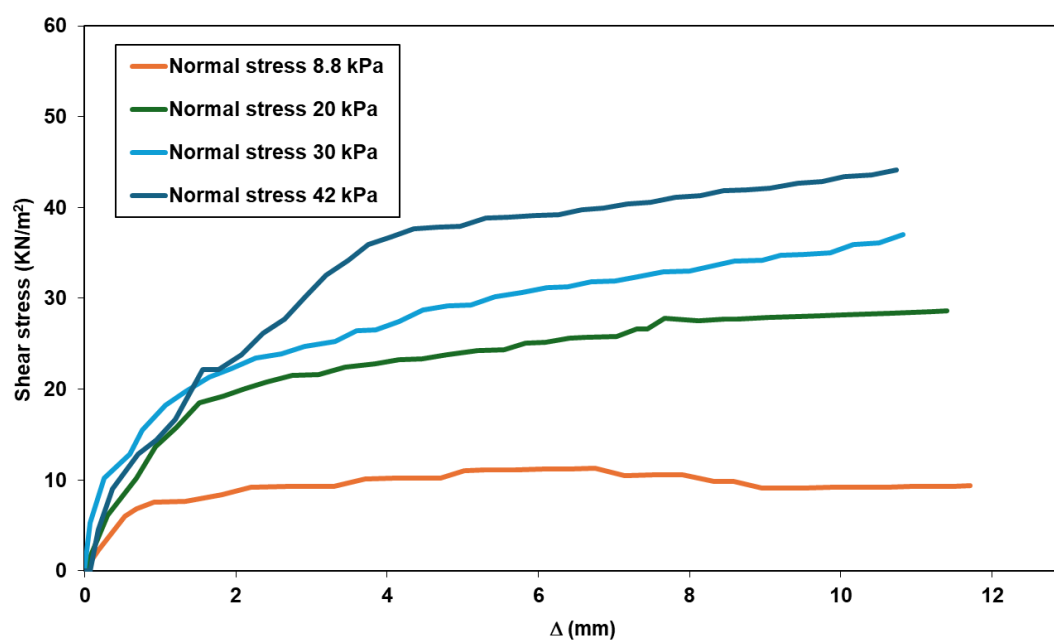


Fig. 19. Shear stresses versus corresponding horizontal displacement for (EPS 30) geofoam–geofoam interface

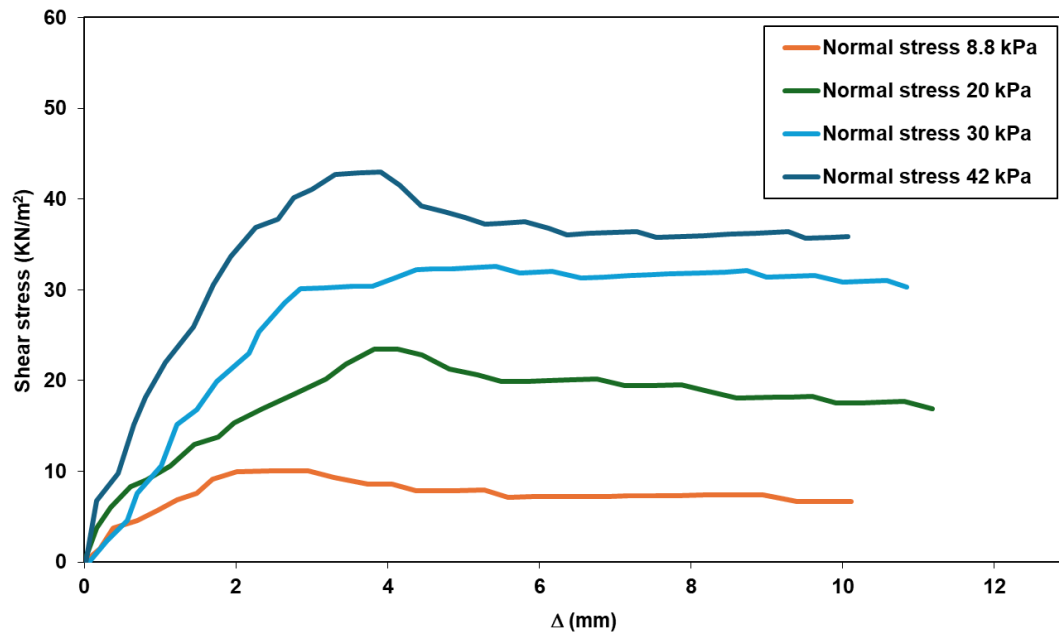


Fig. 20. Shear stresses versus corresponding horizontal displacement for (EPS 30) geofoam–geofoam interface

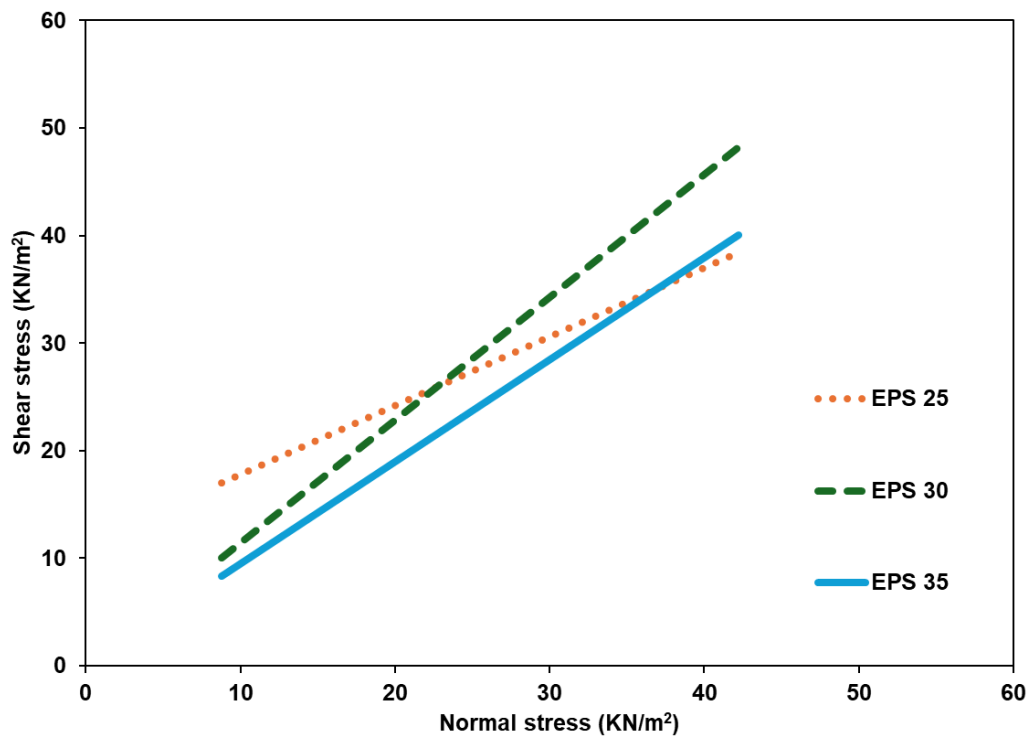


Fig. 21. Failure envelopes of geofoam–geofoam interface

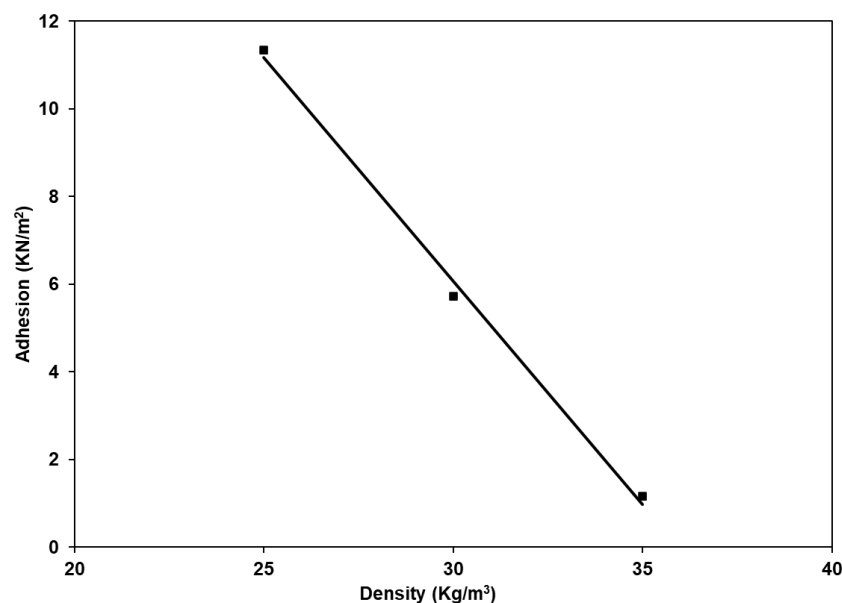


Fig. 22. Relation between geofoam-geofoam interface and adhesion strength

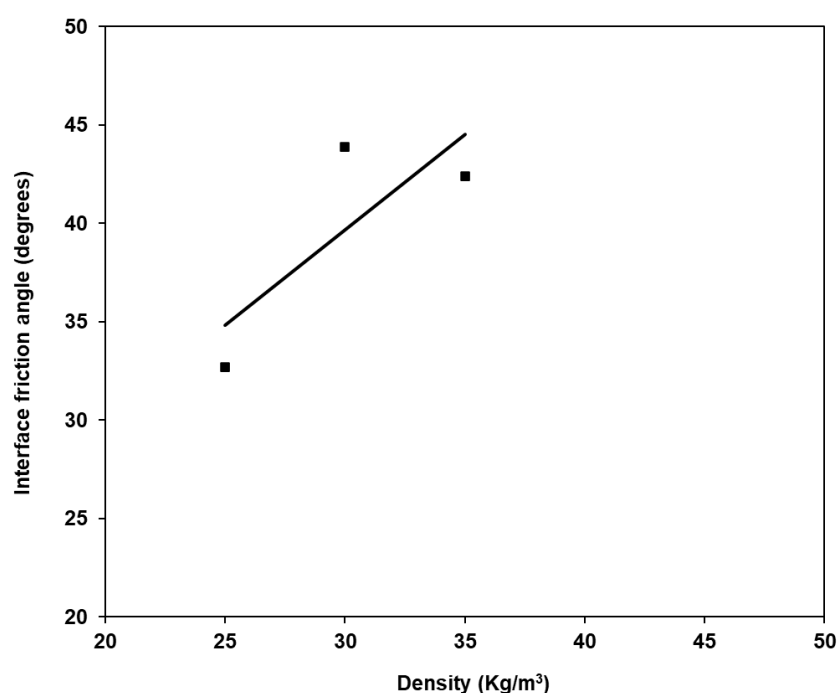


Fig. 23. Relation between geofoam-geofoam interface and interface friction angle

Geofoam – Concrete interface

Fig. 24 to Fig. 26 illustrate the correlation between the shear stress ratio and sample displacement for the geofoam-concrete interfaces, examining three geofoam densities under normal stresses ranging from 8.8 to 42 kPa. The graphs reveal that the shear stress increase rate is the lowest for the low-density (EPS 25) geofoam and increases with increasing geofoam density. All three densities demonstrated a rigid response, as evidenced by the minimal displacement required to achieve the maximum stress ratio. The shear response remained constant at horizontal displacements of approximately 1 mm or less across the investigated normal stress range for all the specimens. However, the shear values exhibited slight

irregularities, potentially due to the non-homogeneity of the concrete surface. The failure envelopes at the interface between the geofoam and concrete for the three examined EPS samples are depicted in Fig. 27. The slopes and intercepts of the failure envelopes were used to determine the contact interface friction angles and corresponding adhesion values. Generally, the friction angles and adhesion values increased with geofoam density. The interface friction angle gradually increased from 28° to 36° when the EPS density increased from 25 to 25 kg/m^3 , with an average internal friction angle of 32.6° , as shown in Fig. 28. Concurrently, along the contact surface, the adhesion exhibited a rapid increase from approximately 0.5 to 3.7 kPa, as shown in Fig. 29.

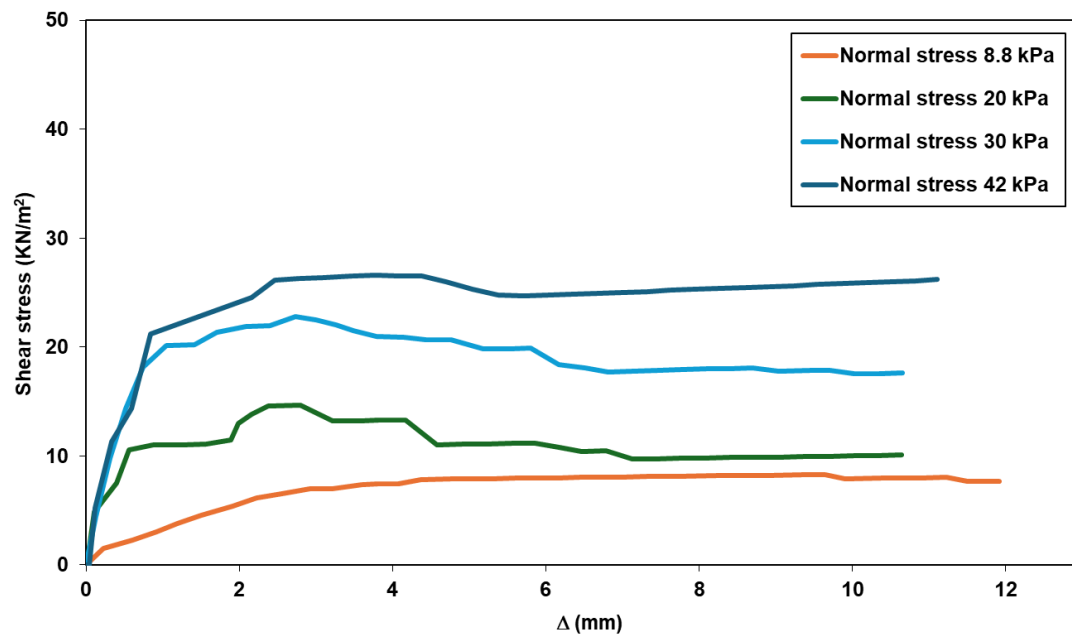


Fig. 24. Shear stresses versus corresponding horizontal displacement for (EPS 25) geofoam–concrete interface

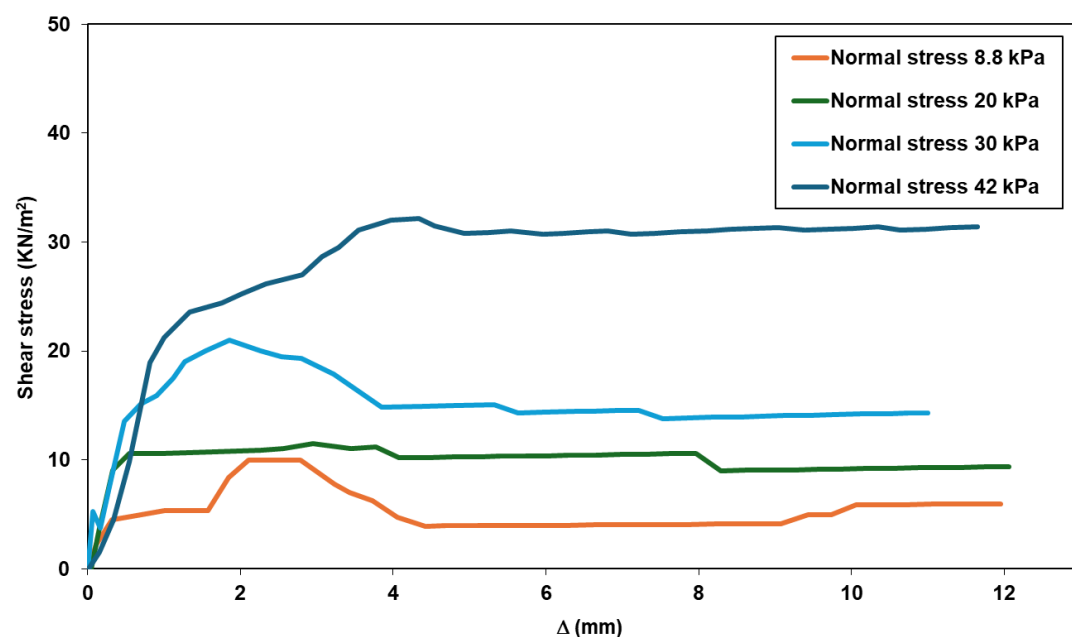


Fig. 25. Shear stresses versus corresponding horizontal displacement for (EPS 30) geofoam–concrete interface

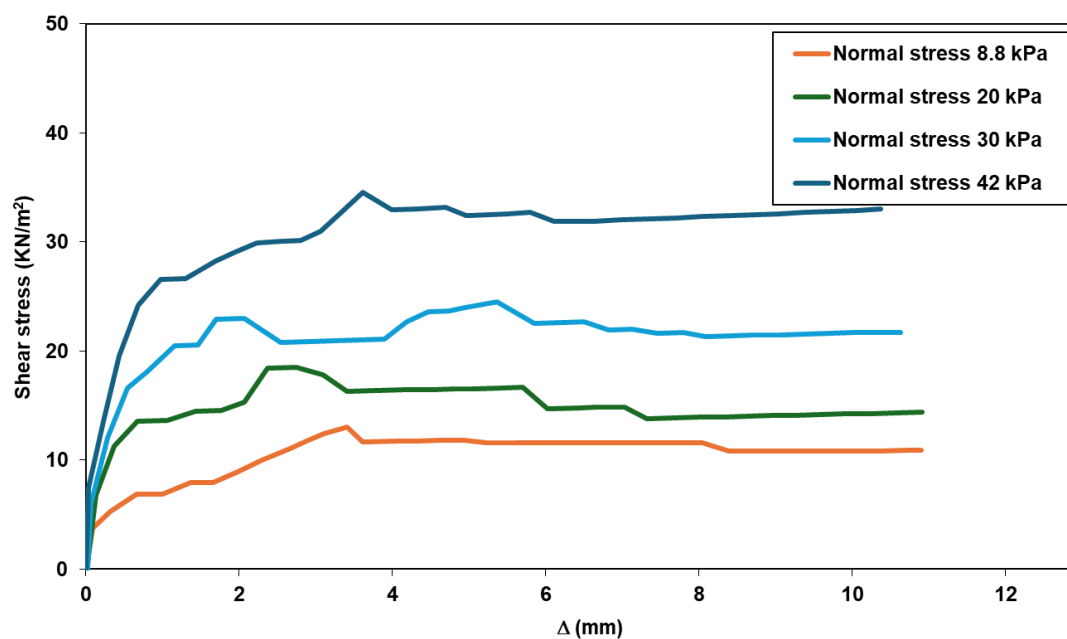


Fig. 26. Shear stresses versus corresponding horizontal displacement for (EPS 35) geofoam–concrete interface

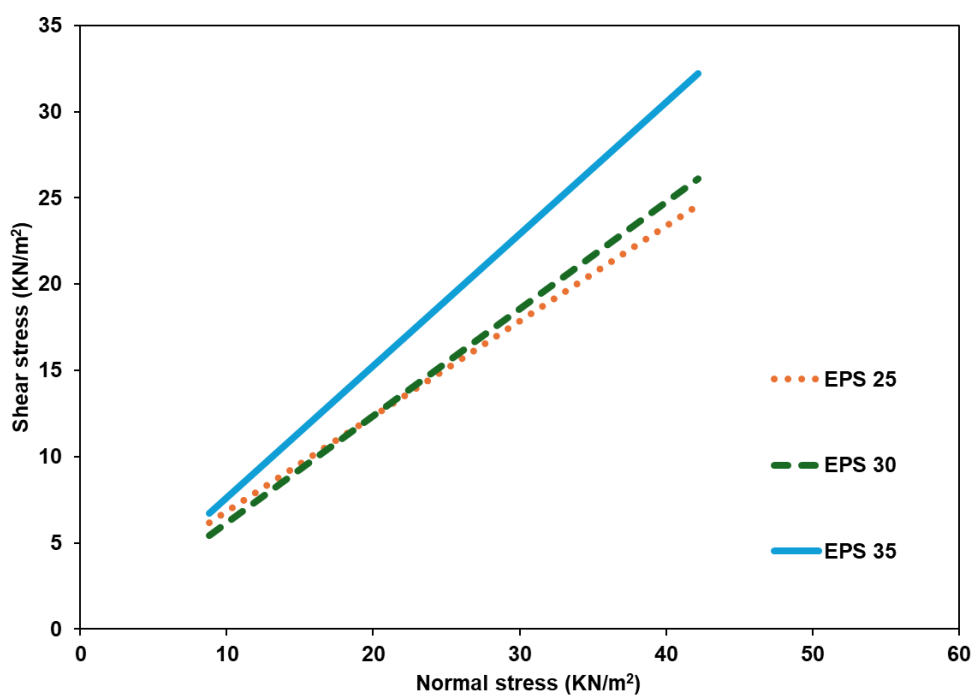


Fig. 27. Failure envelopes of geofoam – concrete interface

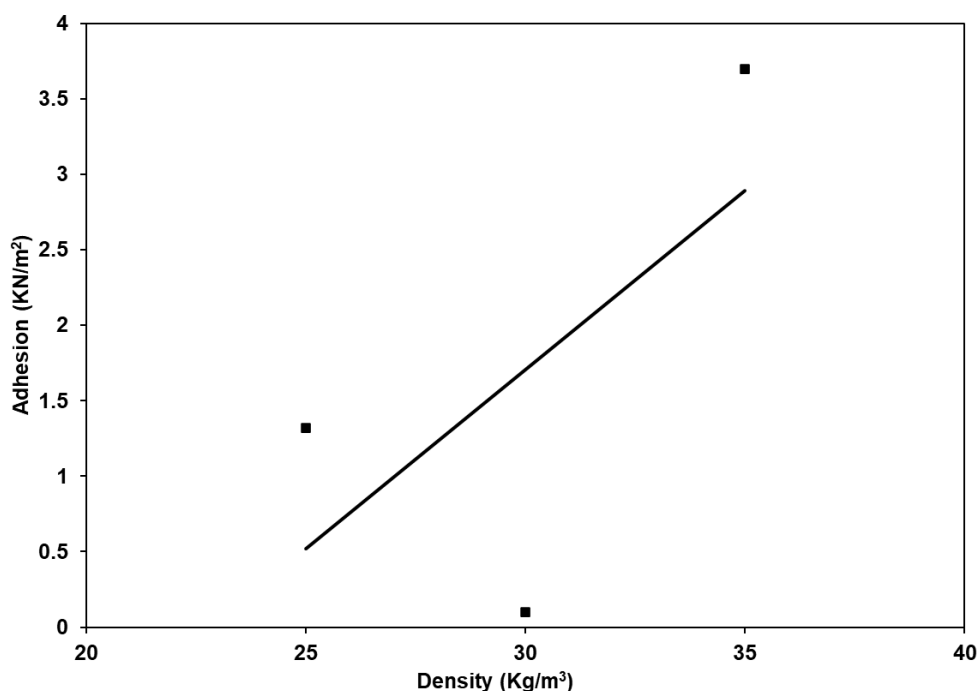


Fig. 28. Relation between geofoam-concrete interface and adhesion strength

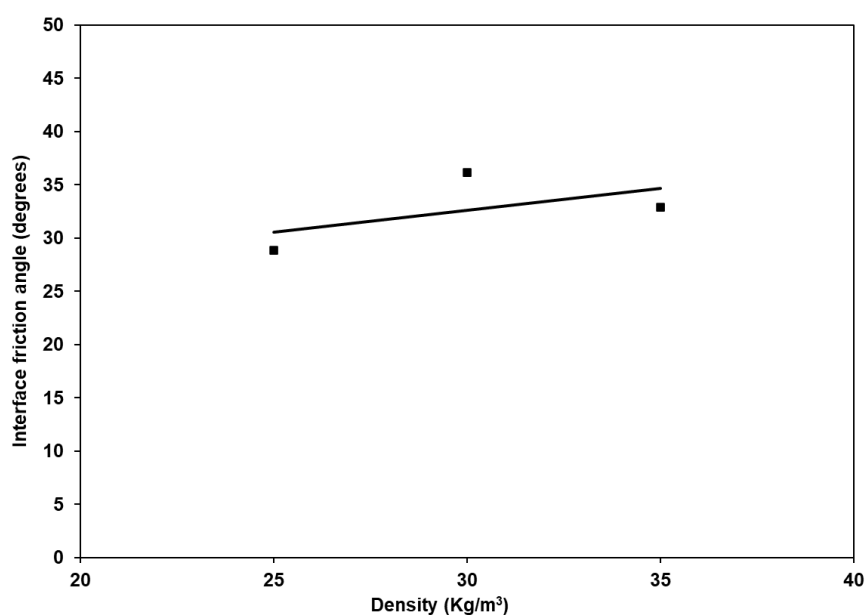


Fig. 29. Relation between geofoam-concrete interface and interface friction angle

Geofoam – Steel interface

The geofoam-steel interactions were analyzed using the shear stress ratio and horizontal displacement correlations for EPS25, EPS30, and EPS35, as shown in Fig. 30 to Fig. 32. All densities exhibited a similar pattern: an initial slow increase in shear stress, followed by a significant increase at displacements below 1 mm, mirroring the behavior observed at the interface of geofoam-concrete. The peak shear stress values showed a slight increase with EPS density increased, reaching 31.6, 32.5, and 38.4 kPa for EPS25, EPS30, and EPS35, respectively. This trend suggests that denser geofoam samples

possess a stronger interface strength when subjected to a given normal stress, which is likely because of the enhanced interaction between the high-density geofoam and the contacting material. Further analysis was performed using linear Mohr-Coulomb failure envelopes to represent the relationship between the geofoam density and interface strength, as shown in Fig. 33. As the geofoam density increased, both the interface angle and the adhesion friction showed notable improvements. Specifically, the adhesion values increased from 8.2 to 10.7 kPa, whereas the interface friction angle increased from 24.2° to 33° see Fig. 34 to Fig. 35. The results highlighted the importance of considering geofoam density when designing and implementing interfaces between geofoam and steel in engineering projects, as higher densities can provide superior strength and stability in such interactions.

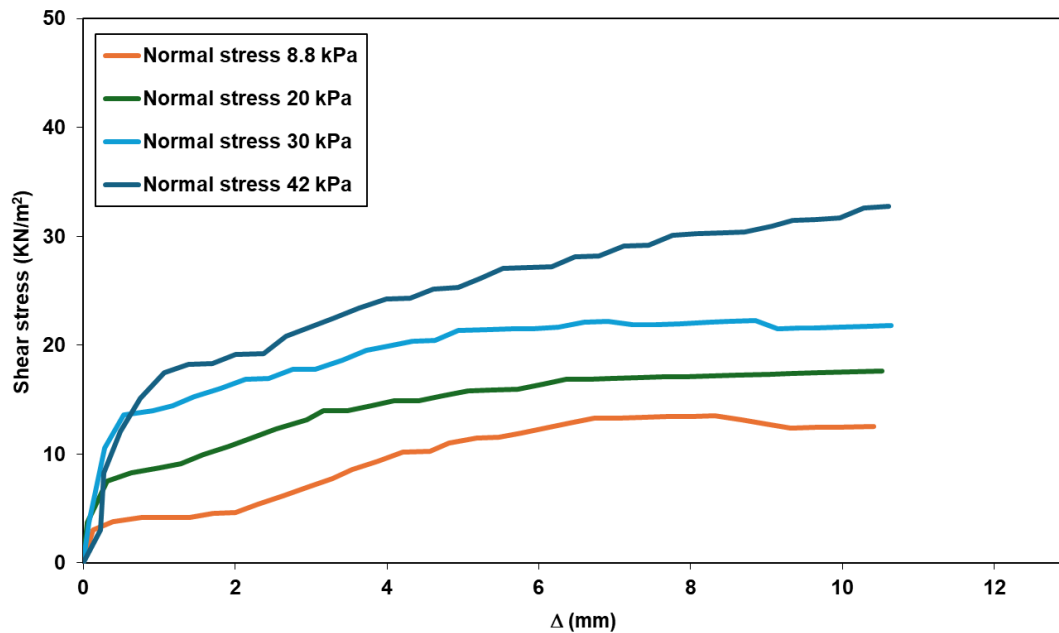


Fig. 30. Shear stresses versus corresponding horizontal displacement for (EPS 25) geofoam–Steel interface

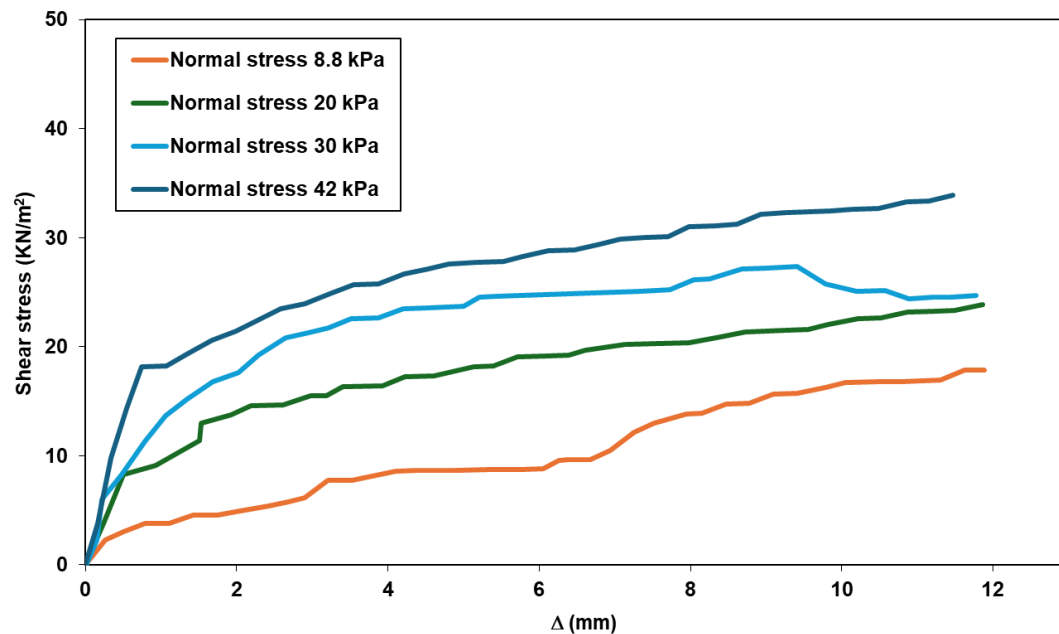


Fig. 31. Shear stresses versus corresponding horizontal displacement for (EPS 30) geofoam–steel interface

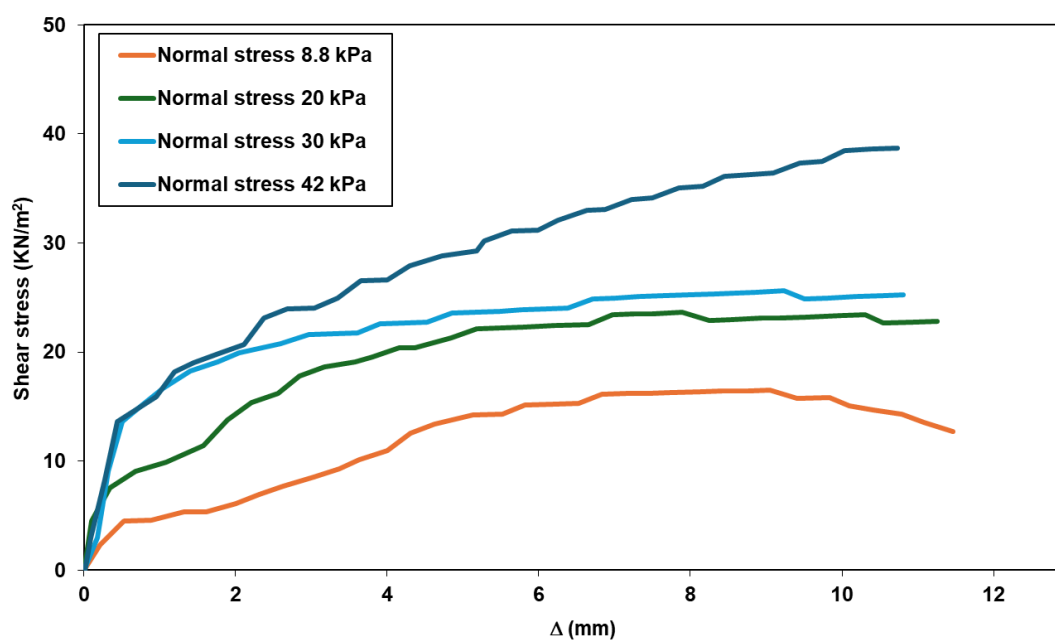


Fig. 32. Shear stresses versus corresponding horizontal displacement for (EPS 35) geofoam–steel interface

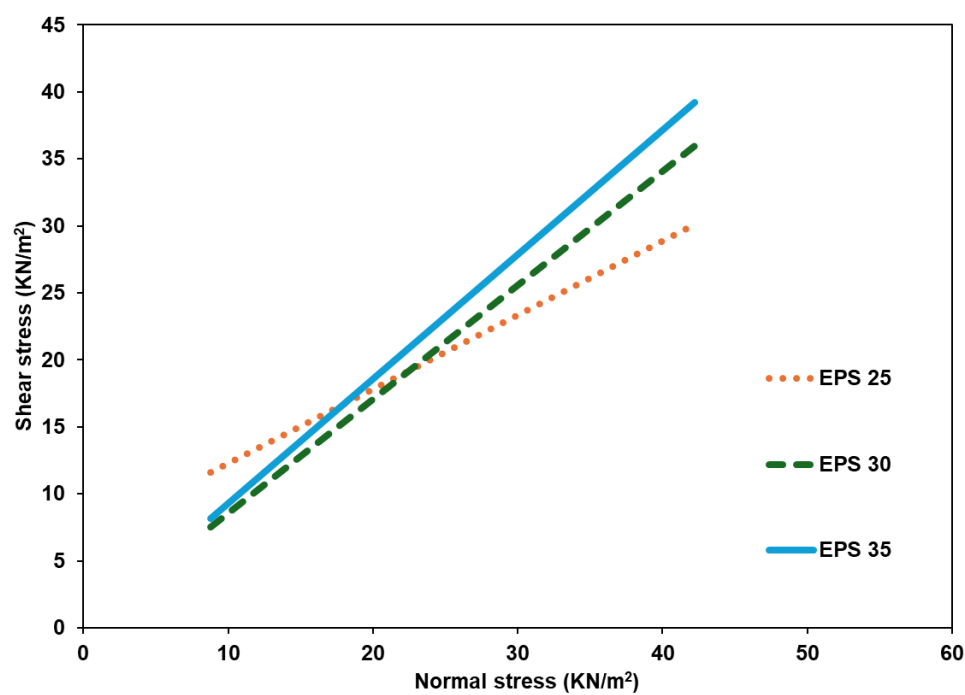


Fig. 33. Failure envelopes of geofoam – steel interface

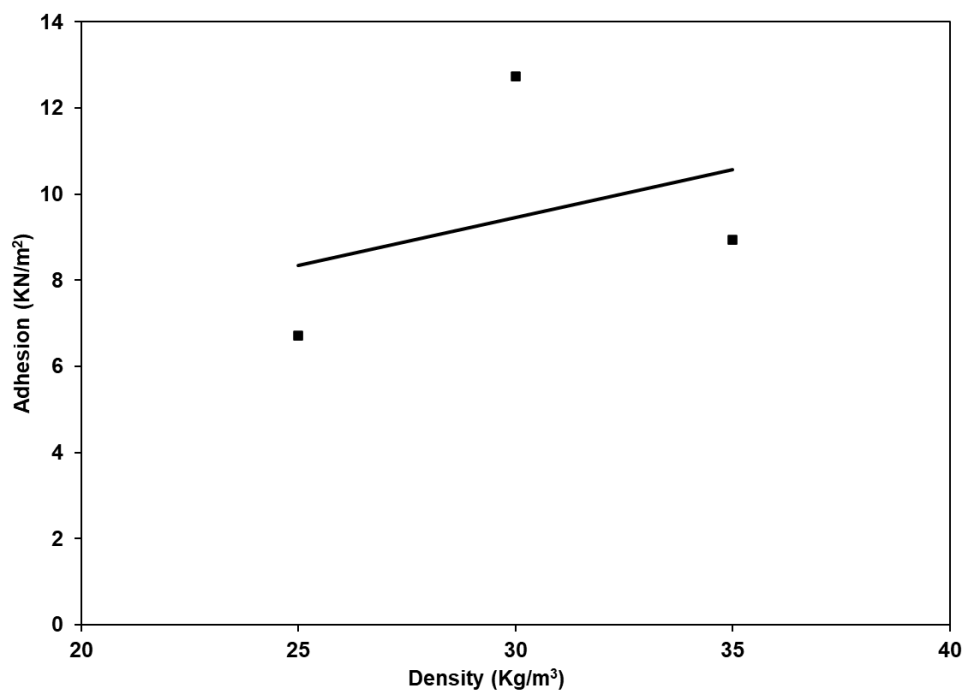


Fig. 34. Relation between geofoam-steel interface and adhesion strength

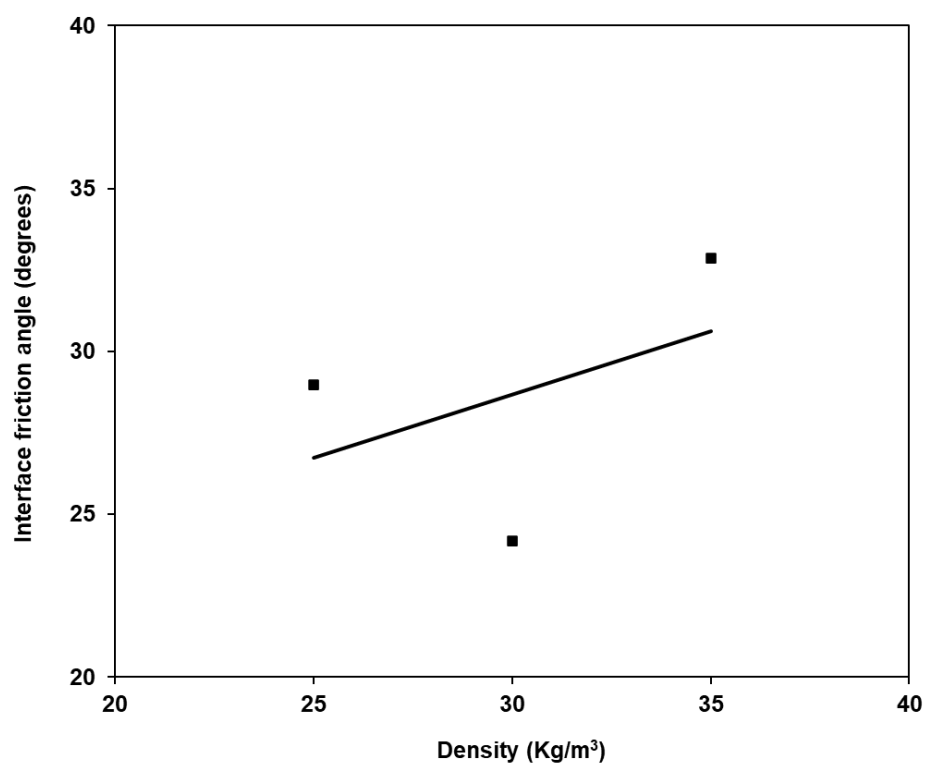


Fig. 35. Relation between geofoam-steel interface and interface friction angle

Table 5. Summary of geofoam interface experimental results.

Interface	Geofoam density (kg/m ³)	Coefficient of friction (tan δ)	
		Measured	Average
Geofoam - Sand	25 - 35	0.45 to 0.63	0.57
Geofoam - Geofoam	25 - 35	0.64 to 0.96	0.83
Geofoam - Concrete	25 - 35	0.55 to 0.73	0.64
Geofoam - Steel	25 - 35	0.55 to 0.65	0.55

4 Conclusion

An extensive investigation of geofoam block behavior was conducted using 67 direct shear tests. The shear strength characteristics of EPS blocks were investigated in this study, focusing on samples with densities of 25, 30, and 35 Kg/m³. Furthermore, shear tests were conducted to assess the interface shear characteristics of EPS geofoam when in contact with sand, steel, and concrete, which are frequently utilized in construction projects. The comprehensive testing program allowed researchers to analyze how the density of geofoam affects its shear strength and frictional properties when in contact with different surfaces. Also, the experimental findings of the current study provide the necessary shear parameters for conducting numerical simulations. This experimental study led to the following conclusions:

1. Under direct shear conditions, the geofoam blocks experienced shear deformation without actual failure. As density increased from 25 to 35 kg/m³, the shear strength increased from 22.75 to 41.4 kPa, indicating a strong dependence on the material cohesion. Nevertheless, as the density increased, the angle of internal friction showed a slight increase from 13.5° to 16.9°.
2. The interface between geofoam and sand exhibited a reduction in adhesion from 4.5 to 0.5 kPa, accompanied by a substantial increase in the interface friction angle from 24° to 32° as the geofoam density increased from 25 to 35 kg/m³. This is due to the fact that in comparison to high-density geofoam materials, the adhesion of low-density geofoam interacts more effectively with sand particles under high normal stresses.
3. Similarly, the interaction between geofoam blocks exhibited a reduction in adhesion from 11.3 to 1.1 kPa, accompanied by a substantial increase in the interface friction angle from 32° to 44° as the geofoam density increased from 25 to 35 kg/m³. This suggests that the interaction between geofoam blocks is primarily determined by the interface friction angle.
4. Geofoam blocks in contact with steel and concrete exhibited an increase in both the internal friction angle and adhesion with increasing geofoam density.

Further research is needed to investigate the interface characteristics between geofoam and various construction materials in wet environments, as well as the impact of different geofoam densities, particularly when geofoam is encased in a geotextile layer.

References

- [1] J. Horvath, "The compressible inclusion function of EPS geofoam," *Geotextiles and Geomembranes*, vol. 15, no. 1–3, pp. 77–120, Jun. 1997, doi: 10.1016/S0266-1144(97)00008-3.
- [2] M. A. Meguid, M. R. Ahmed, M. G. Hussein, and Z. Omeman, "Earth Pressure Distribution on a Rigid Box Covered with U-Shaped Geofoam Wrap," *International Journal of Geosynthetics and Ground Engineering*, vol. 3, no. 2, p. 11, Jun. 2017, doi: 10.1007/s40891-017-0088-4.
- [3] M. A. Meguid, M. G. Hussein, M. R. Ahmed, Z. Omeman, and J. Whalen, "Investigation of soil-geosynthetic-structure interaction associated with induced trench installation," *Geotextiles and Geomembranes*, vol. 45, no. 4, pp. 320–330, Aug. 2017, doi: 10.1016/j.geotextmem.2017.04.004.
- [4] R. J. Bathurst, S. Zarnani, and A. Gaskin, "Shaking table testing of geofoam seismic buffers," *Soil Dynamics and Earthquake Engineering*, vol. 27, no. 4, pp. 324–332, Apr. 2007, doi: 10.1016/j.soildyn.2006.08.003.
- [5] M. I. Khan and M. A. Meguid, "Experimental Investigation of the Shear Behavior of EPS Geofoam," *International Journal of Geosynthetics and Ground Engineering*, vol. 4, no. 2, p. 12, Jun. 2018, doi: 10.1007/s40891-018-0129-7.
- [6] A. H. Padade & J. N. Mandal, "Direct Shear Test on Expanded Polystyrene," 2012.
- [7] A. T. Özer and O. Akay, "Interface Shear Strength Characteristics of Interlocked EPS-Block Geofoam," *Journal of Materials in Civil Engineering*, vol. 28, no. 4, Apr. 2016, doi: 10.1061/(ASCE)MT.1943-5533.0001418.
- [8] F. Wagner G (1986) A senior report on expanded polystyrene as lightweight embankment material. University of New Brunswick, "Expanded polystyrene (EPS) as a lightweight embankment material," 1686.
- [9] H. H. Y. F. (1996) Kuroda S, "Simulation of shaking table test for EPS embankment model by distinct element method. In: Proceedings of international symposium on EPS (expanded poly-styrol) construction method, Tokyo," 1996.
- [10] M. Sheeley and D. Negussey, "An Investigation of Geofoam Interface Strength Behavior," in *Soft Ground Technology*, Reston, VA: American Society of Civil Engineers, Mar. 2001, pp. 292–303. doi: 10.1061/40552(301)23.
- [11] J. C. Barrett and A. J. Valsangkar, "Effectiveness of connectors in geofoam block construction," *Geotextiles and Geomembranes*, vol. 27, no. 3, pp. 211–216, Jun. 2009, doi: 10.1016/j.geotextmem.2008.11.010.
- [12] Miki G, "Ten year history of EPS method in Japan and its future challenges. In: Proceeding of the international symposium on EPS construction method, Tokyo, pp 394–411," 1996.
- [13] Negussey D, "Properties and applications of geofoam, society of the plastics industry. Inc Foamed Polystyrene Alliance, Washington, DC," 1997.
- [14] V. C. Xenaki and G. A. Athanasopoulos, "Experimental Investigation of the Interaction Mechanism at the EPS Geofoam-Sand Interface by Direct Shear Testing," *Geosynth Int*, vol. 8, no. 6, pp. 471–499, Jan. 2001, doi: 10.1680/gein.8.0204.
- [15] D. A. , A. D. K. & M. E. G. Chrysikos, "EPS geofoam surface shear resistance," 2006.
- [16] A. H. Padade and J. N. Mandal, "Interface strength behavior of expanded polystyrene EPS geofoam," *International Journal of Geotechnical Engineering*, vol. 8, no. 1, pp. 66–71, Jan. 2014, doi: 10.1179/1938636213Z.00000000056.
- [17] NRRL, "Expanded polystyrene used in road embankments. NRRL, Oslo," 1992.
- [18] H. Tananda, A. Handoko, and P. P. Rahardjo, "The Use Of Lightweight Material At Road Access Construction On Slope," *Indonesian Geotechnical Journal*, vol. 2, no. 3, pp. 95–108, Dec. 2023, doi: 10.56144/igj.v2i3.61.
- [19] EN 826, "Determination of Compression Behavior of Thermal Insulation Products," 2013.
- [20] ASTM D4245, "Standard Test Methods for Minimum Index Density and Unit Weight of Soils and Calculation of Relative Density 1," 2006.
- [21] ASTM D2487, "Practice for Classification of Soils for Engineering Purposes (Unified Soil Classification System)," May 01, 2011, *ASTM International, West Conshohocken, PA*. doi: 10.1520/D2487-11.
- [22] ASTM D5321, "Test Method for Determining the Shear Strength of Soil-Geosynthetic and Geosynthetic-Geosynthetic Interfaces by Direct Shear," Jan. 01, 2014, *ASTM International, West Conshohocken, PA*. doi: 10.1520/D5321_D5321M-14.
- [23] ASTM D3080, "Test Method for Direct Shear Test of Soils Under Consolidated Drained Conditions," Nov. 01, 2011, *ASTM International, West Conshohocken, PA*. doi: 10.1520/D3080_D3080M-11.